Expansion of the effective action around non-Gaussian theories

OPEN ACCESS
IOP Publishing
Journal of Physics A: Mathematical and Theoretical
J. Phys. A: Math. Theor. **51** (2018) 375004 (35pp)
https://doi.org/10.1088/1751-8121/aad52e

Expansion of the effective action around non-Gaussian theories

Tobias Kühn[1] **and Moritz Helias**[1,2]

[1] Institute of Neuroscience and Medicine (INM-6) and Institute for Advanced Simulation (IAS-6) and JARA BRAIN Institute I, Jülich Research Centre, Jülich, Germany
[2] Department of Physics, Faculty 1, RWTH Aachen University, Aachen, Germany

E-mail: t.kuehn@fz-juelich.de

Received 31 January 2018, revised 20 July 2018
Accepted for publication 23 July 2018
Published 10 August 2018

Abstract

This paper derives the Feynman rules for the diagrammatic perturbation expansion of the effective action around an arbitrary solvable problem. The perturbation expansion around a Gaussian theory is well-known and composed of one-line irreducible diagrams only. For the expansions around an arbitrary, non-Gaussian problem, we show that a more general class of irreducible diagrams remains in addition to a second set of diagrams that has no analogue in the Gaussian case. The effective action is central to field theory, in particular to the study of phase transitions, symmetry breaking, effective equations of motion, and renormalization. We exemplify the method on the Ising model, where the effective action amounts to the Gibbs free energy, recovering the Thouless–Anderson–Palmer mean-field theory in a fully diagrammatic derivation. Higher order corrections follow with only minimal effort compared to existing techniques. Our results show further that the Plefka expansion and the high-temperature expansion are special cases of the general formalism presented here.

Keywords: effective action, non-Gaussian theory, irreducible diagram, Ising model, TAP-approximation

1. Introduction

Many-particle systems are of interest in various fields of physics. Field theory offers a versatile unique language to describe such systems and powerful methods to treat diverse problems arising in classical statistical mechanics, quantum mechanics, quantum statistics, quantum

field theory, and stochastic dynamical systems [1–5]. Diagrammatic techniques in particular are convenient and efficient to organize practical calculations that arise in the context of systematic perturbation expansions and fluctuation expansions around a solvable problem. But most techniques rely on the solvable part being Gaussian: The basic connecting elements in Feynman diagrams, or Mayer graphs [6], are lines. The purpose of this paper is to extend the diagrammatic computation of a central quantity, the effective action Γ, beyond this Gaussian case.

The effective action, vertex generating functional, or Gibbs free energy, is the first Legendre transform of the generating functional of connected Green's functions or cumulants. Originally developed in statistical mechanics to study non-ideal gases in the 1930s, its modern formulation as a Legendre transform was introduced in the context of quantum statistics [7], but has soon been applied in quantum field theory [8] (similar concepts had been developed in parallel in quantum field theory [9]).

The effective action is central to the study of phase transitions, because its stationary points determine the values of the order parameters that characterize the states in which matter may exist; it therefore reduces the problem of a phase transition to finding bifurcation points in a variational problem [2, 3, 5]. This formulation yields self-consistency equations for the mean value of a field that incorporate fluctuation corrections. At lowest order, at the tree level of diagrams, one obtains the mean-field theory of the Curie–Weiss type. Higher Legendre transforms generalize this concept to finding self-consistent solutions for renormalized higher order Green's functions [7][5, chapter 6] [10, 11]; the second transform leading, at lowest order, to a self-consistency equation for the propagator, the Hartree–Fock approximation [12] [5, i.p. chapter 6 for a review].

The second reason for the importance of the effective action is that it compactly encodes all dynamical or statistical properties of a system: connected Green's functions decompose into tree diagrams, whose vertices are formed by derivatives of Γ. Conversely, relatively fewer diagrams contribute to Γ, making its computation favorable: Its perturbative expansion around a Gaussian solvable theory, or around Gaussian fluctuations with regard to a background field, requires only one-line (particle) irreducible graphs (1PI) [2, 3, 7, 13].

Third, treating critical points by renormalization group methods in classical [14, 15] and quantum systems [16] leads to the study of flow equations for the effective action; most explicitly shown in its functional formulation [10, 17, 18].

Perturbative calculations are essential for most applied problems. But practically all techniques in field theory are based on expansions around the Gaussian case. The topic of this article is a systematic, diagrammatic, and perturbative expansion of the effective action in the general case, where the solvable problem is not of Gaussian type; in statistics: the unperturbed problem has cumulants of orders three or higher; in field theory: the bare theory has non-vanishing connected Green's functions of orders three or higher; in diagrams: we have bare propagators that tie together three or more field points instead of or besides the usual propagator lines.

It may be obvious that the linked cluster theorem in this case remains intact without change, shown below for completeness. Also the converse problem, the decomposition of Green's functions into connected Green's functions by Wick's theorem is immediately replaced by its general counterpart, the factorization of moments into all product sets of cumulants [19]. But diagrammatic rules for the direct expansion of the effective action do not follow as simply. Only for particular non-Gaussian cases, diagrammatic rules have been derived earlier: for the classical non-ideal gas [6, 20] and for the Ising model [21, 22] (compare [5, end of chapter 6.3.1]). For the classical gas, one finds that only so called star-graphs contribute [5, 6, 21,

chapter 6.3.2], which is known as Mayer's second theorem. Star-graphs are diagrams that do not fall apart by removing one cumulant. For the Ising model one has to introduce a special notation for the sums, the so called $\mathcal{N}$-form, which only leaves contributions from star graphs [22]. At the end of section 2.6, we will give more details on this result and show its relation to our work.

We first derive a recursive diagrammatic algorithm to compute the effective action perturbatively around a non-Gaussian solvable theory. Then we show that the correction terms produced by the iteration satisfy a set of Feynman rules: Only two topologically defined classes of diagrams remain. The first being irreducible diagrams in a more general sense than in the known Gaussian case. The second being diagrams that contain vertex functions of the solvable theory. The Feynman rules for the former directly follow from the linked cluster theorem. The rules for the latter graphs follow from a set of problem-independent skeleton diagrams that we present subsequently. This set of rules then allows the computation of corrections at arbitrary order in perturbation theory in a non-iterative manner. We find, however, that the iterative procedure itself proves highly efficient. Applied to the special case of the Ising model, it affords only a few more calculations than the method that is specific to the problem [21, 22]. In this particular case, the iterative procedure is closely related to the known high temperature expansion [23].

The remainder of the paper is organized as follows: In section 2.1 we introduce the notation and the minimal extension of the diagrammatic language required. Section 2.2 sets up the general perturbative problem and shows why the expansion of the partition function and the generating functional of connected Green's functions straight forwardly extends to the non-Gaussian setting. These preparations are required to derive in section 2.3 our main result, a recursive algebraic equation that determines Γ. Section 2.4 interprets the algebraic expressions in diagrammatic language, leading to a set of Feynman rules to calculate all graphs contributing to Γ at arbitrary given order in a non-iterative manner. In section 2.5 we exemplify the algorithm for the simplest non-Gaussian extension of a φ^3 theory. In section 2.6 we demonstrate its application to the Ising model (which turns into the Sherrington–Kirkpatrick spin glass model for Gaussian random couplings [24]) to derive the Thouless–Anderson–Palmer mean-field theory [25] and its higher order corrections [21–23, 26, 27] in a purely diagrammatic manner.

2. Results

We here choose a notation that should be transparent with regard to the nature of the problem (following to some extent [13]): our results easily transfer to classical statistical mechanics, quantum mechanics, quantum statistics, or quantum field theory. For clarity, we here stick to the language of classical statistical field theory, in particular to bosonic fields. In the following section 2.1 we set up the language and define elementary quantities.

2.1. Definition of a field theory

We assume that the physical system has degrees of freedom $x \in \mathcal{E}$. We may think of x as a scalar, a vector (as in the example in section 2.6) or a (possibly multi-component) field. The domain $\mathcal{E}$ must be chosen accordingly. The system is described by the action S

$$S : \mathcal{E} \mapsto \mathbb{R}$$

with the property that a particular configuration of x appears with probability $p(x) \propto \exp(S(x))$. The partition function $\mathcal{Z}$ is then given as

$$\mathcal{Z}(j) := \int_x \exp(S(x) + j^{\mathrm{T}}x), \qquad Z(j) := \mathcal{Z}(j)/\mathcal{Z}(0), \tag{1}$$

where we denote as $j^{\mathrm{T}}x$ the inner product on the space $\mathcal{E}$. The symbol $\int_x$ stands for the sum over all configurations of $x \in \mathcal{E}$, which technically may be a sum, an integral, or a path-integral, depending on the space $\mathcal{E}$. We call j the source field. The properly normalized moment-generating function is denoted as $Z(j)$. Its logarithm is the cumulant generating function

$$W(j) := \ln Z(j), \qquad \langle\langle x^n \rangle\rangle(j) := W^{(n)}(j), \tag{2}$$

also called generating functional of the connected Green's functions in field theory; in statistical mechanics it is related to the Helmholtz free energy $F(j) = \ln \mathcal{Z}(j)$ by $W(j) = F(j) - F(0)$. We denote the nth derivative of a function f by $f^{(n)}$ and the nth cumulant as $\langle\langle x^n \rangle\rangle$.

To define the effective action $\Gamma(x^*)$, we eliminate the dependence on the source field j in favor of the mean value $\langle x \rangle$

$$x^*(j) := \langle x \rangle = \langle\langle x \rangle\rangle = W^{(1)}(j), \tag{3}$$

by a Legendre–Fenchel transform

$$\Gamma(x^*) := \sup_j j^{\mathrm{T}}x^* - W(j). \tag{4}$$

We provide the derivation of (4) in appendix A.1, because we need an intermediate step as the starting point of the perturbative expansion. To this end we employ the reciprocity property of Legendre transforms

$$j(x^*) = \Gamma^{(1)}(x^*), \tag{5}$$

which, as derived in the appendix (with (A.2)), leads to the integral-differential equation [13, section 3.23.6]

$$\exp\left(-\Gamma(x^*)\right) = \mathcal{Z}(0)^{-1} \int_{\delta x} \exp\left(S(x^* + \delta x) + \Gamma^{(1)\mathrm{T}}(x^*)\, \delta x\right). \tag{6}$$

The latter expression is the starting point for the perturbative expansion of Γ. It is also the natural starting point of a loopwise expansion. The derivative operators that lead to $W^{(1)}$ and $\Gamma^{(1)}$ are given according to the space $\mathcal{E}$ as either partial derivatives or, in the case of fields, functional derivatives.

2.2. Perturbative problems

The equation of state (5) provides us with a self-consistency equation for the mean value x^*. The general strategy is therefore to obtain an approximation of Γ that includes fluctuation corrections and then use the equation of state to get an approximation for the mean value including these very corrections. We will here derive a perturbative procedure to calculate approximations of Γ and will find the graphical rules for doing so. To solve a problem perturbatively we decompose the action as

$$S(x) = S_0(x) + \epsilon V(x) \tag{7}$$

with a part S_0 that can be solved exactly, that is we know its corresponding cumulant generating function $W_0(j)$, and the remaining terms collected in $\epsilon V(x)$. For the special case of S_0 being quadratic in the fields x, this leads to the well known result that corrections to Γ are composed of one-line irreducible graphs only; our algorithm includes but extends this case to non-quadratic S_0.

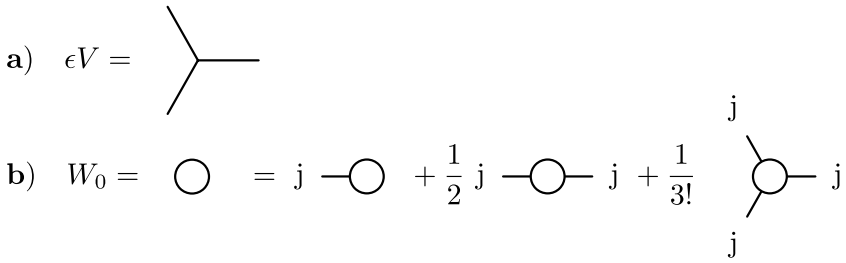

Figure 1. Expansion around a theory with first three non-vanishing cumulants. (a) Bare vertex, here corresponding to a term $\propto x^3$. (b) Cumulants of the solvable part W_0 of the theory: the first three cumulants are non-vanishing, corresponding to circles with one, two, and three legs, respectively.

An example of this situation is depicted in figure 1, where the solvable theory W_0 already contains cumulants of order one to three. We use the common notation for the interaction or bare vertices, which we will call just 'vertices' in the following: the nth power of the field x is denoted as a vertex with n emerging lines. The connecting elements in the graphs are the cumulants contained in W_0. These are symbolized by circles, where the number of legs corresponds to the order of the cumulant (following e.g. [1, 3]). In ordinary Feynman diagrams, W_0 would only have second order cumulants, which are typically denoted by straight lines connecting the vertices.

The proof for the diagrammatic expansion closely follows the proof of the linked cluster theorem (sometimes also called first Mayer theorem [6]), the connectedness of contributions to the cumulant generating function W. We therefore briefly recapitulate the most important steps of the latter proof (adapted from [2, section 6.1.1]) here and provide all details in appendix A.3 for completeness and consistency of notation.

The perturbative corrections $W_V(j) = W(j) - W_0(j)$ to the cumulant generating function obey the operator equation (following from (A.4))

$$\exp(W_V(j)) = \exp\left(-W_0(j)\right) \exp\left(\epsilon V(\partial_j)\right) \exp\left(W_0(j)\right) \frac{\mathcal{Z}_0(0)}{\mathcal{Z}(0)}, \tag{8}$$

where the latter constant factor is immaterial for the determination of cumulants. Expanding in ϵ, the function W can be constructed iteratively, where each step

$$W_{l+1}(j) - W_l(j) = \frac{\epsilon}{L} \left(\exp\left(-W_l(j)\right)\ V(\partial_j)\ \exp\left(W_l(j)\right)\right) + \mathcal{O}\left(\epsilon^2/L^2\right) \tag{9}$$

produces additional diagrams. The proof of connectedness then proceeds by induction under the assumption that all graphs contained in W_l are connected. In the following we will call a 'component' a term that appears in W_V that is composed of a product of vertices, the Taylor coefficients V, and of cumulants $W_0^{(n)}$, the derivatives of the cumulant generating function of the unperturbed theory. Representing V in its Taylor series, every vertex of V ties together components already contained in W_l. The cumulant generating function is then given as

$$W = \lim_{L\to\infty} W_L.$$

Combinatorics shows that only those graphs survive in the limit that pick up each of their k vertices in a different step in (9), from which the factor $\left(\frac{\epsilon}{L}\right)^k \binom{L}{k} \overset{L\to\infty}{\to} \frac{\epsilon^k}{k!}$ arises (for details see appendix A.3).

So we see that W_l at any intermediate step l may contain connected components with arbitrary numbers of external legs. By the inductive nature of the proof it is therefore clear that the linked cluster theorem holds independently of the number of connected components in W_0; that is to say it is generally true, even if already W_0 contains connected components with arbitrary numbers of legs; if it is the cumulant generating function of a non-Gaussian theory.

2.3. Recursion for the effective action

We now proceed to derive our main result, the diagrammatic expansion of the effective action Γ. We here explain the main steps and provide all details in appendices A.4 and A.5.

To lowest order in perturbation theory, setting $\epsilon = 0$ in (7), we get $W(j) = W_0(j)$; the leading order term in Γ is the corresponding Legendre transform

$$\Gamma_0(x^*) = \sup_j j^{\mathrm{T}} x^* - W_0(j). \tag{10}$$

We first need to derive a recursive equation to obtain approximations of the form

$$\Gamma(x^*) =: \Gamma_0(x^*) + \Gamma_V(x^*), \tag{11}$$

where we defined $\Gamma_V(x^*)$ to contain all correction terms that have at least one interaction vertex due to the interaction potential V to some order ϵ^k in perturbation theory. We will use the iteration in a second step to proof Feynman rules for the diagrams.

It is *a priori* not clear that the decomposition (11) is useful. We show in appendix A.4 that this indeed so and, moreover, that it leads to the recursive operator equation for Γ_V

$$\begin{aligned}&\exp(-\Gamma_V(x^*))\\ &= \exp(-W_0(j))\, \exp\left(\epsilon V(\partial_j) + \Gamma_V^{(1)\mathrm{T}}(x^*)(\partial_j - x^*)\right)\, \exp(W_0(j))\big|_{j=\Gamma_0^{(1)}(x^*)},\end{aligned} \tag{12}$$

which has a similar form as (8), defining the linked cluster expansion of W. The term $\Gamma_V^{(1)\mathrm{T}}(x^*)(\partial_j - x^*)$ can hence be seen as a monopole vertex. We want to solve the latter equation iteratively order by order in the number of vertices k, defining $\Gamma_{V,k}$. Analogous to the proof of the linked cluster theorem, we arrive at a recursion by writing the exponential of the differential operator in (12) as a limit and by expanding the logarithm to obtain the iteration

$$g_{l+1}(j) - g_l(j) \tag{13}$$

$$= \frac{\epsilon}{L}\, \exp(-W_0(j) - g_l(j))\, V(\partial_j)\, \exp(W_0(j) + g_l(j)) \tag{14}$$

$$\begin{aligned}&+ \frac{1}{L}\, \exp(-W_0(j) - g_l(j))\, \Gamma_V^{(1)}(x^*)\, (\partial_j - x^*)\, \exp(W_0(j) + g_l(j))\\ &+ \mathcal{O}(L^{-2}),\end{aligned} \tag{15}$$

with initial condition

$$g_0 = 0. \tag{16}$$

We obtain the perturbation correction to Γ (11) as the limit

$$-\Gamma_V(x^*) = \lim_{L\to\infty} g_L(j)\Big|_{j=\Gamma_0^{(1)}(x^*)} =: g(j)\Big|_{j=\Gamma_0^{(1)}(x^*)}. \tag{17}$$

To obtain the final result (17), we need to express $j = \Gamma_0^{(1)}(x^*)$ in $g_l(j)$. The latter step is crucial to obtain $\Gamma_V(x^*)$ as a function of x^*. Because the mean value is given by $x^* = W_0^{(1)}(j_0)$ for $j_0 = \Gamma_0^{(1)}(x^*)$ (following from (3) and (5)), this step effectively expresses all cumulants $\langle\langle x^n \rangle\rangle_0 \equiv W_0^{(n)}$ of the unperturbed theory

$$\langle\langle x^n \rangle\rangle_0(x^*) = W_0^{(n)}(\Gamma_0^{(1)}(x^*)) \tag{18}$$

in terms of the first cumulant $\langle\langle x \rangle\rangle_0(x^*) = x^*$, where x^* is the value of the first cumulant of the full theory. The relation $j_0(x^*)$ can practically be obtained either by inverting $x^* = W_0^{(1)}(j_0)$ or directly as $j_0 = \Gamma_0^{(1)}(x^*)$, if $\Gamma_0(x^*)$ is known explicitly. From the last point follows that the differentiation in (15) with $\Gamma_V^{(1)}(x^*) \equiv \partial_{x^*}\Gamma_V(x^*) = \partial_{x^*}(g \circ \Gamma_0^{(1)}(x^*))$ produces an inner derivative $\Gamma_0^{(2)}$ attached to a single leg of a any unperturbed cumulant $W_0^{(n)}$ contained in g_L. Defining the additional symbol

$\Gamma_0^{(2)}(x^*) =:$ 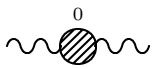

allows us to write these contributions as

$\partial_{x^*}(g \circ \Gamma_0^{(1)}) \equiv (g^{(1)} \circ \Gamma_0^{(1)})\,\Gamma_0^{(2)} =$ 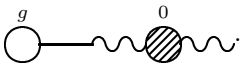

. (19)

This property will become important in the proof that the iteration (13) generates only one-line irreducible graphs. To see this, we have to generalize the notion of irreducibility known from the Gaussian case, which we will do in the following section.

2.4. Proof of a generalized irreducibility

The term 'one-line irredicibility' in the Gaussian case refers to the absence of diagrams that can be disconnected by cutting a single second order bare propagator (a line in the original language of Feynman diagrams). In the slightly generalized graphical notation introduced in figure 1, these graphs would have the form

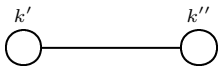

,

where two sub-graphs of k and k' vertices, respectively, are joined by a bare second order cumulant 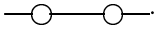 . Before proceeding to the proof, we need to define irreducibility in a more general sense than used in the Gaussian case. If a graph can be decomposed into a pair of sub-graphs both containing vertices by disconnecting the end point of a single vertex, we call this graph reducible. In the Gaussian case, this definition is identical to one-line reducibility, because all end points of vertices necessarily connect to a second order propagator, a line. This is not necessarily the case if the bare theory has higher order cumulants. We may have components of graphs, such as

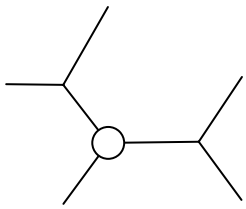 (20)

where the three-point cumulant (could also be of higher order) connects to two third (or higher) order interactions on either side. Disconnecting a single leg, either to the left or to the right, decomposes the diagram into two parts, each of which contains at least one interaction vertex. We call such a diagram reducible and diagrams without this property irreducible here. Note that a single leg of an interaction vertex that ends on a first order cumulant does not make a diagram reducible; both components need to contain at least one interaction.

2.4.1. Cancellation of reducible diagrams. We employ the following graphical notation: Since

$$g_l(j) = :\overset{g_l}{\bigcirc}$$

depends on j only indirectly by the j-dependence of the contained bare cumulants, we denote the derivative by attaching one leg, which is effectively attached to one of the cumulants of W_0 contained in g_l

$$\overset{j}{\text{—}}\overset{g_l}{\bigcirc} := \partial_j \overset{g_l}{\bigcirc} := \partial_j g_l(j).$$

We first note that (13) generates two kinds of contributions to g_{l+1}, corresponding to the lines (14) and (15), respectively. The first line causes contributions that come from the vertices of $\epsilon V(\partial_j)$ alone. These are similar as in the linked cluster theorem (9). Determining the first order correction yields with $g_0 = 0$

$$\begin{aligned} g_1(j) = \frac{\epsilon}{L} &\exp(-W_0(j))\, V(\partial_j)\, \exp(W_0(j)) \\ &+ \mathcal{O}(L^{-2}), \end{aligned} \tag{21}$$

which contains all graphs with a single vertex from V and connections formed by cumulants of W_0. These graphs are trivially irreducible, because they only contain a single vertex.

The proof of the linked cluster theorem (see appendix A.3) shows how the construction proceeds recursively: correspondingly the $l+1$st step (14) generates all connected graphs from components already contained in $W_0 + g_l$. These are tied together with a single additional vertex from $\epsilon V(x)$. In each step, we only need to keep those graphs where the new vertex in (14) joins at most one component from $\boldsymbol{g_l}$ to an arbitrary number of components of W_0, hence we maximally increase the number of vertices in each component by one. This is so, because comparing the combinatorial factors (A.9) and (A.10), contributions formed by adding more than a single vertex (joining two or more components from g_l by the new vertex) in a single step are suppressed with at least L^{-1}, so they vanish in the limit (17).

The second term (15) is similar to (14) with three important differences:

- The differential operator appears in the form $\partial_j - x^*$. As a consequence, when setting $j_0 = \Gamma_0^{(1)}(x^*)$ in the end in (17), all terms cancel where ∂_j acts directly on $W_0(j)$, because $W_0^{(1)}(j_0) = x^*$; non-vanishing contributions only arise if the ∂_j acts on a component contained in g_l. Since vertices and cumulants can be composed to a final graph in arbitrary order, the diagrams produced by $\partial_j - x^*$ acting on g_l are the same as those in which $\partial_j - x^*$ first acts on W_0 and in a subsequent step of the iteration another ∂_j acts on the produced $W_0^{(1)}$. So to construct the set of all diagrams it is sufficient to think of ∂_j as acting on g_l alone; the reversed order of construction, where ∂_j first acts on W_0 and in subsequent steps of the iteration the remainder of the diagram is attached to the resulting $W_0^{(1)}$, is contained in the combinatorics.

- The single appearance of the differential operator ∂_j acts like a monopole vertex: the term therefore attaches an entire sub-diagram contained in $\Gamma_V^{(1)}$ by a single link to any component contained in g_l.
- These attached sub-diagrams from $\Gamma_V^{(1)}(x^*)$ do not depend on j; the j-dependence of all contained cumulants is fixed to the value $j = \Gamma_0^{(1)}(x^*)$, as seen from (12). As a consequence, these sub-graphs cannot form connections to vertices in subsequent steps of the iteration.

Considering that $\Gamma_V^{(1)}(x^*)$ is represented by (19), in step $l+1$ the line (15) contributes graphs of the form

$$g^{(1)}\,\Gamma_0^{(2)}\,g_l^{(1)} = \tag{22}$$

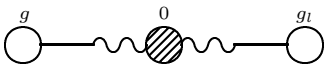

Since by their definition as a pair of Legendre transforms we have

$$1 = \Gamma_0^{(2)} W_0^{(2)} =$$

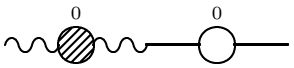

we notice that the subtraction of the graphs (22) may cancel certain connected graphs produced by the line (14). In the case of a Gaussian solvable theory W_0 this cancellation is the reason why only one-line irreducible contributions remain. We here obtain the more general result, that these contributions cancel all reducible components, according to the definition above. We will prove this central result in the following.

To see the cancellation, we note that a reducible graph by our definition has at least two components joined by a single leg of a vertex. Let us first consider the case of a diagram consisting of exactly two irreducible sub-diagrams joined by a single leg, as it is generated by (15). This leg may either belong to the part $g^{(1)}$ or to $g_l^{(1)}$ in (22), so either to the left or to the right sub-diagram. In both cases, there is a second cumulant $W_0^{(2)}$ either left or right of $\Gamma_0^{(2)}$. This is because if the two components are joined by a single leg, this particular leg must have terminated on a $W_0^{(1)}$ prior to the formation of the compound graph; in either case this term generates $W_0^{(1)} \overset{\partial_i}{\to} W_0^{(2)}$.

The second point to check is the combinatorial factor of graphs of the form (22). To construct a graph of order k, where the left component has k' bare vertices and the right has $k-k'$, we can choose one of L steps within the iteration in which we may pick up the left term by (15). The remaining $k-k'$ vertices are picked up by (14), which are $\binom{L-1}{k-k'}$ possibilities to choose $k-k'$ steps from $L-1$ available ones. Every addition of a component to the graph comes with L^{-1}. Any graph in Γ_V with k' vertices is $\propto \frac{\epsilon^{k'}}{k'!}$, so together we get

$$\frac{L}{L}\frac{\epsilon^{k'}}{k'!}\left(\frac{\epsilon}{L}\right)^{k-k'}\binom{L-1}{k-k'} \overset{L\to\infty}{\to} \frac{\epsilon^k}{k'!(k-k')!}. \tag{23}$$

The symmetry factors s_1, s_2 of the two sub-graphs generated by (22) enter the symmetry factor $s = s_1 \cdot s_2 \cdot c$ of the composed graph as a product, where c is the number of ways in which the two sub-graphs may be joined. But the factor s, by construction, excludes those symmetries that interchange vertices between the two sub-graphs. Assuming, without loss of generality, a single sort of interaction vertex, there are $s' = \binom{k}{k'} = \frac{k!}{k'!(k-k')!}$ ways of choosing k' of the k vertices to belong to the left part of the diagram. Therefore the symmetry factor

s is smaller by the factor s' than the symmetry factor of the corresponding reducible diagram constructed by (14) alone, because the latter exploits all symmetries, including those that mix vertices among the sub-graphs. Combining the defect s' with the combinatorial factor (23) yields $\frac{1}{k'!(k-k')!}/s' = \frac{1}{k!}$, which equals the combinatorial factor of the reducible graph under consideration.

The generalization to the case of an arbitrary number of sub-diagrams of which M are irreducible and connected to the remainder of the diagram by exactly one link, called 'leaves', is straightforward: we can always pick one of these sub-diagrams and replace it by its corresponding contribution to $\Gamma^{(1)}(x^*)$. Then, by the same arguments as before, we produce the same diagram with the same prefactor, only with opposite sign. In summary we conclude that all reducible graphs are canceled by (22). We therefore obtain the first part of our Feynman rules: All connected, irreducible diagrams that are also contained in the perturbation expansion of W_V also contribute to Γ_V with a negative sign and the same combinatorial factor.

But there is a second sort of graphs produced by (22) that does not exist in the Gaussian case: If the connection between the two sub-components by  ends on a third or higher order cumulant. These graphs cannot be produced by (14), so they remain with a minus sign. We show an example of such graphs in figure 4(c). One might wonder why this contribution does not cancel, while making a 'reducible impression', if one interprets $\Gamma_0^{(2)}$ as a kind of two-point interaction. The solution is that for diagrams of this kind, indeed contributions of opposite signs and same absolute values are generated, but the contribution with the one sign is generated once and the contribution with the other sign twice, therefore the total contribution does not vanish. We address this issue more thoroughly in appendix A.7.

Moreover, subsequent application of ∂_{x^*} on such components produces graphs that contain higher order derivatives of $\Gamma_0^{(n)}$. By the arguments given in the proof for the generalized irreducibility, we deduce that all diagrams cancel that have at least one leaf from $W_V^{(1)}$ (that includes only unperturbed cumulants and interactions, but no vertices $\Gamma^{(n)}(x^*)$) and that is connected to the remainder of the diagram by a single leg of an interaction (and not via a leg of $\Gamma^{(n)}(x^*)$, see appendix A.7). Reducible non-standard diagrams that violate these prerequisites can occur. In the end of the following subsection, we will also give an example for this case. To enumerate all all non-standard diagrams and to find their Feynman rules, we also derive a set of skeleton diagrams in the following subsection that allow the computation of all contributions at any given order including their combinatorial factor.

2.4.2. Perturbative diagrammatics derived from skeleton diagrams. To obtain a better understanding of the types of diagrams that contribute to the perturbation expansion, in particular the non-standard diagrams not contained in W_V, it is useful to derive a non-iterative approach based on a set of skeleton diagrams. We use the term 'skeleton diagram' for a diagram containing dressed as opposed to bare cumulants and vertices. We start with a Taylor expansion around a adroitly chosen point x_1

$$\Gamma(x^*) = \Gamma(x_1) + \Gamma^{(1)}(x_1)^{\mathrm{T}}(x^* - x_1) + \sum_{n=2}\sum_{i_1\cdots i_n} \frac{\Gamma^{(n)}_{i_1\cdots i_n}(x_1)}{n!} \prod_{l=1}^{n}(x^* - x_1)_{i_l}, \tag{24}$$

where we wrote the first two terms explicitly. We now choose a particular point x_1 by making use of the involutive property of the Legendre transform, which is given for all smooth and convex cumulant generating functions, irrespective of the form of the underlying theory. Concretely, we choose $x_1 := W^{(1)}(\Gamma_0^{(1)}(x^*))$, which is equivalent to

$$\begin{array}{rclcrcl} j_0 & = & \Gamma_0^{(1)}(x^*) & \Longleftrightarrow & x^* & = & W_0^{(1)}(j_0) \\ j_0 & = & \Gamma^{(1)}(x_1) & & x_1 & = & W^{(1)}(j_0). \end{array} \tag{25}$$

As an immediate consequence, we see that

$$x^* - x_1 = W_0^{(1)}(j_0) - W^{(1)}(j_0) = -W_V^{(1)}(j_0). \tag{26}$$

Using these relations and the definition of the Legendre transform, the two terms in the first line of (24) can be rewritten as

$$\begin{aligned} & j_0^{\mathrm{T}} x_1 - W(j_0) + j_0^{\mathrm{T}}(x^* - x_1) \\ & = j_0^{\mathrm{T}} x^* - W_0(j_0) - W_V(j_0) \\ & = \Gamma_0(x^*) - W_V(j_0). \end{aligned} \tag{27}$$

We now see that the first two terms in (24), besides $\Gamma_0(x^*)$, also contain all diagrams from $W_V(j_0)$, but with the opposite sign. We note that by their dependence on x^* and j_0, respectively, these contributions can be calculated: The relation (25) allows us to express all bare cumulants $W_0^{(n)}(j_0)$ that appear in $-W_V$ in terms of the first cumulant $x^* \equiv W_0(j_0)$.

The second line in (24) produces additional diagrams that are of second order in the interaction or higher; this is because the 'leaves' (26) of these tree diagrams are $-W_V$, which, by definition, contain at least one interaction vertex. These terms include those diagrams that cancel the reducible diagrams included in $W_V(j_0)$, as proven above. In addition, these terms contain the non-standard diagrams. We will describe in the following, how the exact form and combinatorial factors of these diagrams can be obtained.

To express the dressed vertex functions $\Gamma^{(n)}(x_1)$ that appear in the second line of (24), we first derive a perturbative expansion for $\Gamma^{(2)}(x_1)$, which is basically Dyson's equation. We here include the derivation to see that it holds beyond the Gaussian case. Decomposing W into the solvable part and its perturbative corrections, the reciprocity relation

$$W^{(2)}(j_0)\,\Gamma^{(2)}(W^{(1)}(j_0)) = 1 \tag{28}$$

takes the form

$$(W_0^{(2)}(j_0) + W_V^{(2)}(j_0))\,\Gamma^{(2)}(\underbrace{W^{(1)}(j_0)}_{\equiv x_1}) = 1.$$

Multiplying from left with $\Gamma_0^{(2)}(W_0^{(1)}(j_0)) = \Gamma_0^{(2)}(x^*)$, which is the inverse of $W_0^{(2)}(j_0)$, we obtain by rearranging

$$\Gamma^{(2)}(x_1) = \Gamma_0^{(2)}(x^*) - \Gamma_0^{(2)}(x^*)\,W_V^{(2)}(j_0)\,\Gamma^{(2)}(x_1). \tag{29}$$

The latter term contains at least one interaction vertex in W_V, the former is of order zero. So we may iterate this equation to obtain an inverted Dyson's equation for $\Gamma^{(2)}$ that reads

$$\Gamma^{(2)}(x_1) = \Gamma_0^{(2)}(x^*) - \Gamma_0^{(2)}(x^*)\,W_V^{(2)}(j_0)\,\Gamma_0^{(2)}(x^*) \pm \dots$$

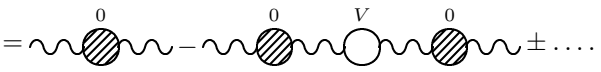

$$\pm \dots . \tag{30}$$

It is easily checked by insertion that (30) solves (29).

So we have expressed the second order vertex at x_1 by means of quantities that are directly accessible or can be calculated perturbatively in a straight-forward way, by their dependence on x^* and j_0, respectively. Higher order vertices are determined in the standard way by differentiating the reciprocity relation (28) multiple times with respect to j_0, and removing the legs $W^{(2)}(j_0)$ that arise from inner derivatives by multiplication with the corresponding inverse $\Gamma^{(2)}(x_1)$. The result is the well-known decomposition of vertex in terms of tree skeleton diagrams [1, 2]

$$\begin{aligned}
\Gamma^{(3)}_{123}(x_1) &= -\sum_{\{i_l\}} W^{(3)}_{i_1 i_2 i_3}(j_0)\,\Gamma^{(2)}_{i_1 1}(x_1)\,\Gamma^{(2)}_{i_2 2}(x_1)\,\Gamma^{(2)}_{i_3 3}(x_1) \\
\Gamma^{(4)}_{1234}(x_1) &= -\sum_{\{i_l\}} W^{(4)}_{i_1 i_2 i_3 i_4}(j_0)\,\Gamma^{(2)}_{i_1 1}(x_1)\,\Gamma^{(2)}_{i_2 2}(x_1)\,\Gamma^{(2)}_{i_3 3}(x_1)\,\Gamma^{(2)}_{i_4 4}(x_1) \\
&\quad + \sum_{\{i_l\}} W^{(3)}_{i_1 i_2 i_3}\,W^{(3)}_{i_4 i_5 i_6}(j_0)\,\Gamma^{(3)}_{i_1 1}(x_1)\,\Gamma^{(2)}_{i_2 2}(x_1)\,\Gamma^{(2)}_{i_3 i_4}(x_1)\,\Gamma^{(2)}_{i_5 3}(x_1)\,\Gamma^{(2)}_{i_6 4}(x_1) + 2\,\text{perm.} \\
&\quad \ldots .
\end{aligned} \tag{31}$$

Diagrammatically, the first of these relations reads

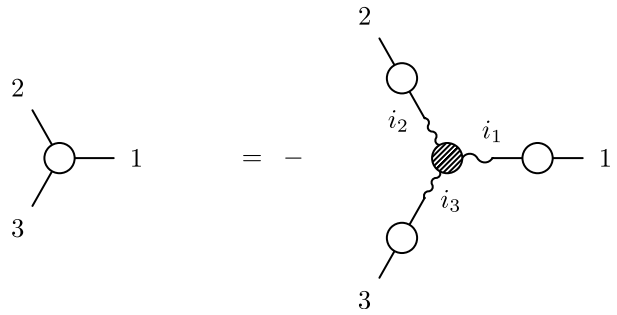

We can hence express vertices of arbitrary order at the point x_1 by cumulants at the point j_0 (which is given by x^* by means of (25)) and $\Gamma^{(2)}(x_1)$, which is again given by the same cumulants and $\Gamma^{(2)}_0(x^*)$ by Dyson's equation (30). The important point to note here is that the set of rules to translate skeleton diagrams into their perturbative expansion is problem independent; it just results from the properties of the Legendre transform and the decomposition into solvable part and perturbation.

Because both factors in every term of the sum in the second line of (24) depend on the interaction V, the order of each such term is the sum of the orders of its factors. We derive two additional rules from this view. First, since also $W_0(j_0)$ and $\Gamma_0(x^*)$ form a pair of Legendre transforms, their reciprocity relation $W^{(2)}_0(j_0)\,\Gamma^{(2)}_0(x^*) = 1$ gives rise to a relation corresponding to (31), but with $\Gamma^{(n)}(x_1)$ replaced by $\Gamma^{(n)}_0(x^*)$ and $W^{(n)}(j_0)$ by $W^{(n)}_0(j_0)$. This means that the lowest order terms for the nth derivative in (31) resum to $\Gamma^{(n)}_0(x^*)$. The final set of skeleton diagrams derived from (24), the main result of this section therefore reads

$$\begin{aligned}
\Gamma(x^*) &= \Gamma_0(x^*) - W_V(j_0) \\
&\quad + \sum_{n=2} \frac{\Gamma^{(n)}_0(x^*) + \bar{\Gamma}^{(n)}(x_1)}{n!}\,(-W^{(1)}_V(j_0))^n,
\end{aligned} \tag{32}$$

where we defined $\bar{\Gamma}^{(n)}(x_1) := \Gamma^{(n)}(x_1) - \Gamma_0^{(n)}(x^*)$, which contains all diagrams from (30) and (31) that have at least one interaction vertex, so which are of order $\mathcal{O}(\epsilon)$ or higher.

The second rule follows from $W_V^{(1)}(j_0)$ being of first order or higher, so that at the nth order in the interaction, we have to consider at most the nth term in the sum in (32). In this last term we must in addition drop the $\bar{\Gamma}$-term. The only term to consider at second order, for example, is

$$\frac{1}{2!} W_V^{(1)}(j_0)^{\mathrm{T}} \Gamma^{(2)}(x_1) W_V^{(1)}(j_0) = \frac{1}{2!} W_V^{(1)\mathrm{T}}(j_0) \Gamma_0^{(2)}(x^*) W_V^{(1)}(j_0) + \mathcal{O}\left(\epsilon^3\right).$$

This term cancels the contributions of the diagrams (b) and (c) in figure 3. However, that all reducible diagrams cancel can be seen more systematically by the constructive arguments given in section 2.4.1.

But equation (27) is useful to get a handle on the non-standard diagrams. If we want to know all such diagrams of a certain order k in the interaction, we first assign the number of interactions to be contained in each factor in any term $\Gamma^{(n)}(x_1)/n! \left(-W_V^{(1)}(j_0)\right)^n$, $2 \leqslant n \leqslant k$ so that they sum up to k. Assigning 0 interaction vertices to $\Gamma^{(n)}$ reduces it to $\Gamma_0^{(n)}(x^*)$, as said above. For non-zero numbers of vertices in $\bar{\Gamma}^{(n)}$, we decompose the latter via (30) and (31) into an expression only containing full cumulants and $\Gamma_0^{(2)}(x^*)$ and distribute again the number of interactions assigned to $\bar{\Gamma}^{(n)}$ among these cumulants. Each full cumulant is then broken down into all its perturbative expansion, for which the standard Feynman rules hold according to the linked cluster theorem (see appendix A.3). Throughout this expansion, we skip all diagrams that are also contained in $-W_V$, because these are just the reducible ones that we know to cancel each other.

Another insight we gain by (32) in combination with (30) is that non-standard diagrams are not necessarily irreducible—in fact, they can even be reducible in the sense that they fall into two parts both containing interactions if we cut a second-order cumulant. We show an example for this phenomenon in a toy model at the end of section 2.5.

2.4.3. Summary of Feynman rules for the non-Gaussian case. We now summarize the algorithmic rules derived from the above observations to obtain Γ:

(i) Calculate $\Gamma_0(x^*) = \sup_j j^{\mathrm{T}} x^* - W_0(j)$ explicitly by finding j_0 that extremizes the right hand side. At this order $g_0 = 0$.

(ii) At order k in the perturbation expansion:

   (a) add all irreducible graphs in the sense of the definition above that have k vertices;

   (b) add all graphs containing derivatives $\Gamma_0^{(n)}$ as connecting elements that cannot be reduced to the form of a graph contained in the expansion of $W_V(j_0)$; the graphs left out are the counterparts of the reducible ones in $W_V(j_0)$. The topology and combinatorial factors of these non-standard contributions are generated iteratively by (13) from the previous order in perturbation theory; this iteration, by construction, only produces diagrams, where at least two legs of each $\Gamma_0^{(n)}$ connect to a third or higher order cumulant. We can also directly leave out diagrams, in which a subdiagram contained in W_V is connected to the remainder of the diagram by a single leg of an interaction vertex. Alternatively, the additional diagrams can be constructed directly for any order k by instantiating the skeleton diagrams generated by (32) to the desired

order, as explained in section 2.4.2. Note that here diagrams may appear in which $\Gamma^{(n>2)}$ couples to less than two third or higher order cumulants. After decomposing all $\Gamma^{(n>2)}$ into $\Gamma_0^{(2)}$ and diagrams from $W^{(n)}$ by (31) and (30), we can discard diagrams, in which at least one subdiagram from W_V forms a leave that is connected by a single link of an interaction vertex; these cancel by the same argument as given in the iterative approach.

(iii) assign the factor $\frac{\epsilon^k}{r_1!\cdots r_{l+1}!}$ to each diagram with r_i-fold repeated occurrence of vertex i; assign the combinatorial factor that arises from the possibilities of joining the connecting elements as usual in Feynman diagrams (see examples below and e.g. [3]);

(iv) express the j-dependence of the nth cumulant $\langle\langle x^n \rangle\rangle(x^*)$ in all terms by the first cumulant $x^* = \langle\langle x \rangle\rangle = W_0^{(1)}(j_0)$; this can be done, for example, by inverting the last equation or directly by using $j_0 = \Gamma_0^{(1)}(x^*)$; express the occurrence of $\Gamma_0^{(2)}$ by its explicit expression.

This set of Feynman rules constitutes the central result of our work. Note that the rules include the well-known Gaussian case, because irreducibility in the here-defined sense is identical to one-line-irreduciblity in the expansion around a Gaussian theory: every leg of an interaction vertex necessarily connects to a line there. Non-standard diagrams hence cannot appear in this case.

The Feynman rules hold for any order k. So one may compute corrections at order k directly without having computed any lower order. The combinatorial factor is fixed unambiguously, too. To get an intuitive understanding of the cancellation, it is still useful to illustrate the recursive construction of graphs in section 2.5 in the application to a minimal, non-Gaussian setting. In section 2.6 we demonstrate the application to systems of Ising spins, recovering the TAP approximation [25], the high temperature expansion [23], and the Plefka expansion [28]. It turns out that the recursive algorithmic procedure leads to a dramatic decrease of required computations.

2.5. Illustrative example for the graphical rules

As a first example let us consider a zero-dimensional field theory, that is to say, a probability distribution of a scalar variable. By assumption, S_0 constitutes the solvable theory, so that $W_0(j)$ can be determined exactly by (2). We here illustrate the method for a solvable theory that has non-vanishing cumulants of orders one, two, and three, hence W_0 is a polynomial of order three

$$W_0(j) = \overset{0}{\bigcirc} = \sum_{n=1}^{3} \langle\langle x^n \rangle\rangle_0 \frac{j^n}{n!},$$

where the cumulants $\langle\langle x^n \rangle\rangle_0$ with $n \in \{1, 2, 3\}$ appear as Taylor coefficients. Its graphical representation is shown in figure 1(b). As perturbation we assume a three point vertex $\epsilon V(x) = \epsilon x^3$, shown in figure 1(a).

According to step (i) we determine $\Gamma_0(x^*)$ by (4), which amounts to the calculation of the derivative $\partial_j W_0(j_0) - x^* = 0$ which determines $j_0(x^*)$.

We now calculate the diagrams recursively according to step (ii). At order $l = 0$ we have $g_0 = 0$. At first order $l = 1$, we therefore get from (21) the graphs shown in figure 2.

Each graph has a single vertex, thus we get a factor $\frac{\epsilon}{1!}$. The combinatorial factors for each graph are stated explicitly above. So the diagrams in Γ_V at first order are identical to all connected diagrams with a single vertex; in this regard, the expansion is identical to the well

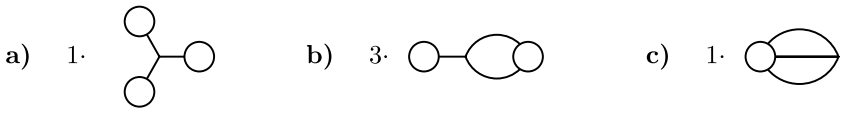

Figure 2. All diagrams contributing to g_1 at first order $l = 1$ generated by (21) for the theory of figure 1.

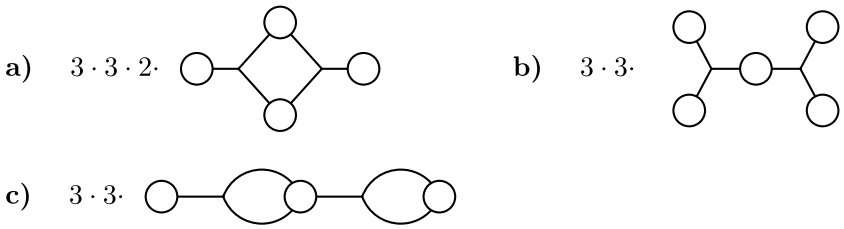

Figure 3. Some diagrams generated by (14) contributing to $g_2 - g_1$ at order $l = 2$. Diagrams (b) and (c) are reducible, so they will drop out.

known Gaussian case, except that the diagram figure 2(c) would not appear in the absence of third order cumulants of the solvable theory.

At order $l = 2$, the graphs in $W_0 \cup g_1$ contain those that have been produced in the previous step. The step (14) therefore produces additional diagrams out of these components, some of which are shown in figure 3.

The diagrams (a) and (b) in figure 3 are composed of the diagram (a) in figure 2 contained in g_1 and one additional vertex. The diagram (c) in figure 3 is composed of diagram (b) in figure 2; its combinatorial factor $3 \cdot 3$ is the combined factor of the first order diagram and the factor 3 due to three possibilities to select a leg of the vertex. We here skipped further diagrams; in particular all diagrams, that are generated by the first order diagram (c) in figure 2.

The line (15) produces additional diagrams with negative sign. We here indicate the simplification $= 1$ by an overbrace. Some diagrams are shown in figure 4.

We observe that the diagram (a) in figure 4 cancels the diagram (b) in figure 3. This cancellation is of the ordinary type; the diagram (b) in figure 3 is one-line irreducible in the original sense: its two components are connected by a second order cumulant, which would be denoted by a line ⎯ in the original graphical language of Feynman diagrams; here denoted as .

An example of the more general cancellation appears between diagram (b) in figure 4 and (c) in figure 3: the two components in figure 3(c) are not connected by a second order cumulant, hence the diagram is not one-line irreducible in the original sense, but it is reducible in the sense we defined above. We see that it is canceled by figure 4(b), consistent with the general proof. If we want to obtain the diagrams of the next order, note that we have to keep reducible diagrams, because the cancellation occurs only after setting $j = \Gamma_0^{(1)}(x^*)$.

The diagram figure 4(c) produced by (15) cannot be generated by (14), because the connecting proper (effective) vertex $\Gamma_0^{(2)} =$ connects to two third order cumulants. It is generated in two ways; with two $\Gamma^{(1)}(x^*)$-components or only one of them. These two contributions have opposite signs, but different prefactors, therefore they do not cancel (see also appendix A.7 for details). We now derive the appearance of this latter diagram by the application of the method using skeleton diagrams. The relevant skeleton diagram is the one that appears at second order on the Taylor expansion in the second line of (24)

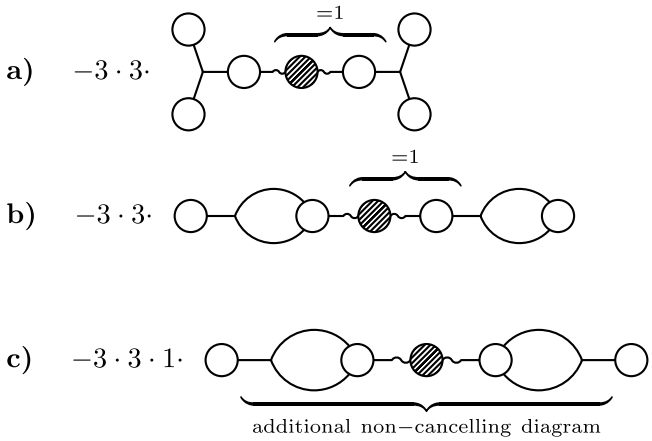

Figure 4. Some diagrams generated by (15) at second order $l = 2$. Diagram (a) and (b) cancel reducible graphs (b) and (c) in figure 3, respectively.

$$\frac{1}{2!} \quad \cdot \tag{33}$$

We now instantiate this diagram with perturbative expansions of the desired order, so that the resulting diagram is of order two: The two point vertex function, by Dyson's equation (30) to lowest order is $\Gamma^{(2)}(x_1) = \Gamma_0^{(2)}(x^*) + \ldots$. The leaves $-W_V^{(1)}$ attached to either side, to first order, contain contributions of the form

$$+\ldots, \tag{34}$$

where all elements on the right are cumulants of the unperturbed system and bare interaction vertices. The combinatorial factor of this latter sub-diagram is computed with the standard rules for connected diagrams, which yields a factor 3 from the possible ways of attaching the first order cumulant to the interaction vertex. There is only a single possibility to attach the additional external leg to the third order cumulant and only a single way to join the elements in the skeleton diagram in (33), besides the explicit factor $1/2!$.

Finally, each remaining diagram must be interpreted algebraically by steps (iii) and (iv). These steps are straight forward here. We note that this step is possible at all in the technique using the skeleton diagrams, because all cumulants appearing are $W_0^{(n)}(j_0) = W_0^{(n)}(\Gamma_0^{(1)}(x^*))$ and in Dyson's equation (30) in addition only $\Gamma_0^{(2)}(x^*)$ appears; so all elements, by assumption of S_0 being the solvable theory, are known. There is yet another observation that we can make in the framework of of this toy model, namely that there are reducible non-standard diagrams that contribute to Γ_V. One example is the following fourth-order cumulant emerging from the $n = 2$ term in the sum in (27) and using the first-order correction from (30) (with second order correction in the interaction for $W_V^{(2)}$):

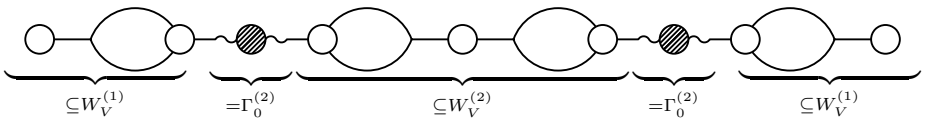

2.6. Application to the Ising model

We here illustrate the method on a simple system, the classical Ising model with the action

$$S(x) = \frac{\epsilon}{2} x^{\mathrm{T}} J x + j^{\mathrm{T}} x, \tag{35}$$

where $x \in \{-1, 1\}^N$ is a vector of Ising spins and J a symmetric matrix with $J_{ii} = 0$. Note that there is no additional constraint on J; it could, for example, be drawn from a random distribution, as done in spin-glass models. In particular there is no restriction to nearest-neighbour interactions. We are here interested in the weak coupling limit with small ϵ.

There are essentially two different ways to arrive at an approximation of the effective action $\Gamma(x^*)$. The first approach represents the pairwise coupling term as the result of a Gaussian average over auxiliary variables (see e.g. [1, chapter 4.3, equation (4.50a)], [5, chapter (5.2) and equation (5.49)], [29, equations (4) and (5)], or [30]). This Hubbard–Stratonovich transform reduces the calculation of $\mathcal{Z}$ to the summation of nth moments of the Gaussian employing Wick's theorem, weighted by the Taylor coefficients of $V(x) = \ln \sum_{x_i} e^{j_i x_i} = \sum_i \ln\, 2\cosh j_i$; the latter play the role of vertices here. Consequently, standard Feynman diagrammatic rules apply. This approach is only applicable to this model because the interaction is pairwise; interactions of higher order cannot be written by help of Gaussian auxiliary fields.

The second way, which we will follow here, considers as the solvable part the single-spin term of the action

$$S_0(x) = j^{\mathrm{T}} x; \qquad W_0(j) = \sum_i \ln\, 2\, \cosh(j_i), \tag{36}$$

which is directly summable, yielding a cumulant-generating function W_0 whose decomposition into a sum over individual sites shows their statistical independence. For each i, the solvable theory therefore has the infinitely many non-vanishing cumulants of a binary variable. The interaction is in turn treated as the perturbation

$$V(x) = \frac{\epsilon}{2} x^{\mathrm{T}} J x. \tag{37}$$

This approach has been followed in quite a number of variations over decades (see e.g. [5, section 5.2 and equation (5.47)], [21, 23, 26–28, 31–33], [34, chapter 3]); these methods agree inasmuch as they all perform an expansion of Γ, where (37) is treated as a perturbation and (36) as the solvable part. In particular this approach is identical to Plefka's method [28].

Both routes of course lead to identical results. To second order in ϵ one obtains the mean-field theory presented by Thouless, Anderson, and Palmer (TAP) [25] as a 'fait acompli', without proof, but mentioning a previous diagrammatic derivation. Indeed, Vasiliev and Radzhabov ([21, 22], summarized in [5, sections 6.3.1, 6.3.2 and 6.3.4]) had derived this result diagrammatically with the help of the analog to the Dyson Schwinger equation for the effective action [35] before (see [5, section 5.2] for a review of this method).

If one performed a perturbation expansion directly on the level of $\mathcal{Z}$ (A.4)

$$\mathcal{Z}(j) = \exp(V(\partial_j))\, \exp(W_0(j)) = \Big\langle \sum_{n=0}^{\infty} \frac{1}{n!} \big(\frac{\epsilon}{2} x^{\mathrm{T}} J x\big)^n \Big\rangle_0, \tag{38}$$

with $\langle f(x)\rangle_0 = \sum_x f(x)\, \exp(j^{\mathrm{T}} x)$, one would quickly obtain unwieldy expressions; but most of these terms cancel by the subsequent transformations $\mathcal{Z} \overset{\ln}{\to} W \overset{\mathcal{L}}{\to} \Gamma$ in the final result, making a direct expansion of Γ desirable. The calculation of Γ at higher orders in ϵ by this direct approach has prompted for computer algebra systems [26]. Georges and Yedidia [23, 33] developed a sequence of shortcuts and tricks for this problem by which they managed the

approximation up to forth order (reviewed in [34, chapter 3]). As mentioned, Γ has been derived diagrammatically by Vasiliev and Radzhabov [21, equation (21)]. Using Dyson–Schwinger equations, they explicitly presented all orders up to and including the third.

We here chose this model to exemplify the application of the general framework exposed in previous sections. For one, because it allows the comparison to a wealth of methods developed over decades, as mentioned above. And also because the Ising model has proven useful in many other applications than micromagnetism, for example artificial neural networks [36]. Especially the TAP-approximation and its higher order corrections are employed to derive analytical approximations [37] to contrastive divergence [38], a learning rule commonly employed to train restricted Boltzmann machines [39, 40]. Another major field, in which the Ising model is applied, are inference problems, where the inverse Ising problem has to be solved, that is, the sources h_i and couplings J_{ij} have to be computed for given means and pairwise covariances. Depending on the problem, the spins represent activities of neural units [41–43], active or inactive genes in the case of gene regulatory networks or participants in financial markets (see [44] for an excellent review of the inverse Ising problem). The most natural quantity for this type of problem would be the second Legendre transform, the usual entropy of the multi-variate binary distribution for given first two moments, because the couplings and sources turn out to be the extrema of this quantity. We present an iterative method to compute the second Legendre transform in appendix A.6. Still, the first Legendre seems to be commonly used also for the inverse problem [27, 45]. The reason for this might be that calculating the second Legendre transform is technically challenging; nevertheless, specific approximations exist that are valid for small correlations, first computed by a technique specialized to the Ising model [46], later obtained by techniques borrowed from the functional renormalization group [47], using the Wetterich equation [17]. An extension to more than pairwise coupling (37) is desirable in these fields [48–50]. In particular the Hubbard–Stratonovich method mentioned above would not work in these cases, while the here proposed approach does.

Performing the here presented diagrammatic expansion, we observe a drastic decrease of computations and their transparent organization by diagrams. The calculation up to fourth order indeed takes only minor effort.

We start with the unperturbed theory, given by (36), in which all spins decouple and the cumulants up to fourth order read

$$\begin{aligned}
\langle\!\langle x_i \rangle\!\rangle_0 &= \langle x_i \rangle_0 = m_i := \tanh(j_i) \\
\langle\!\langle x_i x_j \rangle\!\rangle_0 &= \delta_{ij} \left(1 - m_i^2\right) \\
\langle\!\langle x_i x_j x_k \rangle\!\rangle_0 &= -\delta_{ij}\delta_{jk} 2 m_i \left(1 - m_i^2\right) \\
\langle\!\langle x_i x_j x_k x_l \rangle\!\rangle_0 &= -\delta_{ij}\delta_{jk}\delta_{kl} 2 \left(1 - 3m_i^2\right)\left(1 - m_i^2\right).
\end{aligned}$$

To zeroth order the Legendre transform of W_0 is the entropy of a binary variable

$$\Gamma_0(m) = -\sum_i \frac{1+m_i}{2} \ln\left(\frac{1+m_i}{2}\right) + \frac{1-m_i}{2} \ln\left(\frac{1-m_i}{2}\right), \tag{39}$$

where $(1 \pm m_i)/2$ are the probabilities for $x_i = \pm 1$. The result (39) follows from step (i) of the algorithm by a short calculation from (36); the form is moreover clear, because the distribution (36) maximizes the entropy and the Legendre transform to Γ just fixes j so that the mean is $\langle x_i \rangle = m_i$.

To obtain corrections to (39) we represent the nth cumulant by an empty circle with n legs and the nth derivative of Γ_0 by a hatched circle with n legs. An interaction J_{ij} is denoted by an edge:

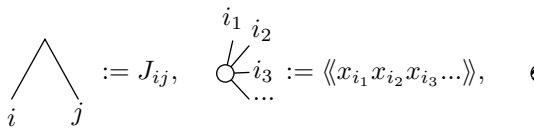

(40)

To evaluate the diagrams, we will only need the second derivative $\Gamma^{(2)}_0$, either directly given by differentiating (39) twice or by using the relation $W^{(2)}_0 \Gamma^{(2)}_0 = 1$. Both yields $\Gamma^{(2)}_{0,ij} = \frac{\delta_{ij}}{1-m_i^2}$. Within this language, the perturbative corrections up to the third order to be added to (39) are readily constructed from steps ii–iv at the end of section 2.4:

$$= \frac{1}{2} \sum_{i \neq j} J_{ij} m_i m_j \tag{41}$$

$$= \frac{1}{2!2^2} 2 \sum_{i \neq j} J_{ij}^2 \left(1 - m_i^2\right) \left(1 - m_j^2\right) \tag{42}$$

$$= \frac{1}{3!2^3} 2^3 \sum_{i \neq j \neq k \neq i} J_{ij} J_{jk} J_{ki} \left(1 - m_i^2\right) \left(1 - m_j^2\right) \left(1 - m_k^2\right) \tag{43}$$

$$= \frac{1}{3!2^3} 2^2 \sum_{i \neq j} J_{ij}^3 \left(-2m_i\right) \left(1 - m_i^2\right) \left(-2m_j\right) \left(1 - m_j^2\right). \tag{44}$$

For the third order diagrams, the symmetry factors 2^3 and 2^2 are noted separately in front of the respective terms. For all diagrams, they are determined as usual for Feynman diagrams (see appendix A.8). Until this order only the first sort of ordinary diagrams composed of vertices and cumulants contribute. All diagrams are irreducible in the general sense defined above.

Going to fourth order, we first consider the four diagrams that are formed out of vertices and cumulants alone. These would also contribute to an expansion of W.

$$= \frac{S_{\mathrm{R}}}{4!2^4} \sum_{i \neq j \neq k \neq l \neq i} J_{ij} J_{jk} J_{kl} J_{li} \left(1 - m_i^2\right) \left(1 - m_j^2\right) \left(1 - m_k^2\right) \left(1 - m_l^2\right) \tag{45}$$

$$= \frac{S_{\mathrm{TM}}}{4!2^4} \sum_{i \neq j \neq k \neq i} J_{ik} J_{ij}^2 J_{kj} \left(-2m_i\right) \left(1 - m_i^2\right) \left(-2m_j\right) \left(1 - m_j^2\right) \left(1 - m_k^2\right) \tag{46}$$

$$= \frac{S_{\mathrm{dC}}}{4!2^4} \sum_{i \neq j} J_{ij}^4 \left(-2\right) \left(1 - 3m_i^2\right) \left(1 - m_i^2\right) \left(-2\right) \left(1 - 3m_j^2\right) \left(1 - m_j^2\right). \tag{47}$$

In the appendix, appendix A.8, we show that the symmetry factors are given by $S_{\mathrm{R}} = 48$, $S_{\mathrm{TM}} = 96$ and $S_{\mathrm{dC}} = 8$. The fourth standard diagram is shown below. It is similar to the first

and second non-standard contribution. To indicate the origin of the different contributions, we denote sub-graphs originating from $\Gamma^{(1)}$ by filled circles—they are, however, translated in the same way as the empty ones:

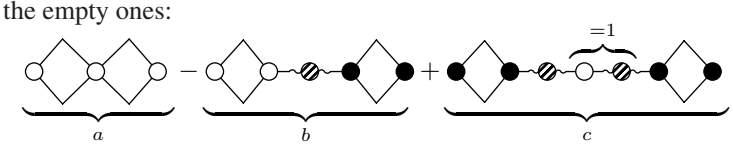

$$
\begin{aligned}
&= \frac{1}{2^4} \sum_{i\neq j\neq k} J_{ij}^2 J_{jk}^2 \\
&\times \left[\frac{S_a}{4!} \left(1-m_i^2\right)(-2)\left(1-m_j^2\right)\left(1-3m_j^2\right)\left(1-m_k^2\right) \right. \\
&\left. - \left(1-m_i^2\right) \frac{(-2m_j)\left(1-m_j^2\right)(-2m_j)\left(1-m_j^2\right)}{\left(1-m_j^2\right)} \left(1-m_k^2\right) \left(\frac{S_b}{3!} - \frac{S_c}{2!} \right) \right]
\end{aligned}
\tag{48}
$$

With the symmetry factors given by $S_a = 48$, $S_b = 24$ and $S_c = 4$ (see appendix, section appendix A.8 for the derivation), we can add up the contributions of the three diagrams, which gives, leaving out factors that are equal in all diagrams for simplicity:

$$
\frac{1}{4!} 48 (-2)\left(1-3m_j^2\right) + \left(-\frac{8}{2!1!} + \frac{1}{2} 4 \right) 4m_j^2 = -4\left(1-m_j^2\right).
$$

The last term looks like a second cumulant and, interestingly, this contribution is indeed exactly canceled by the contribution of the ring-diagram of fourth order (45) in the case that exactly one pair of indices, which belong to cumulants represented at opposite sites of the ring, are equal.

This has to be so, as shown by Vasiliev and Radzhabov [22], because, according to their terminology, diagram *a* is a 'nonstar graph', that is, not a star graph—it decomposes into two parts by removing a cumulant (a 'vertex' in their words). Note that the star graph property implies irreducibility, but not vice versa. As Vasiliev and Radzhabov have shown, only star diagrams contribute to the effective action of the Ising model, if we introduce so called compensating graphs. These graphs are constructed as follows: Take all star graphs of a certain order and draw contractions (in [22] depicted by dashed lines) in all possible ways between circles that are not connected by an interaction and therefore represent indices that could take the same value (keep in mind that $J_{ii} = 0$). If two or more circles are contracted, they are considered as a single circle, are associated with a common index and are translated as the product of all cumulants associated to this point. Then substract all compensating graphs that are non-star-graphs and sum up original and compensating graphs [22, equation (8)]. We may check that our result is consistent with this rule. In the ring-diagram (45), the only contraction that leads to a non-star graph is the one that identifies the indices of two opposite circles. This contribution therefore cancels from the final expression for the effective action, analogous to the summed up contributions of the diagrams *a*, *b*, and *c*. In our framework, not only the double Citroën diagram (47) contributes to the sum over only two unequal indices, but also the ring diagram in the case that the indices of pairwise opposite circles and the diagrams *a*, *b* and *c* in the case that the indices of the outmost circles are equal (see appendix A.8 for details). In summary, the general method that we present here is consistent with the specific result known for the Ising model.

In total, we obtain the following expression for the effective action in an Ising model with coupling J_{ij}:

$$-\Gamma(\boldsymbol{m}) \tag{49}$$

$$\begin{aligned}
&= -\sum_i \frac{1+m_i}{2}\ln\left(\frac{1+m_i}{2}\right) + \frac{1-m_i}{2}\ln\left(\frac{1-m_i}{2}\right) \\
&\quad + \frac{1}{2}\epsilon\sum_{i\neq j} J_{ij}m_i m_j + \frac{1}{4}\epsilon^2\sum_{i\neq j} J_{ij}^2\left(1-m_i^2\right)\left(1-m_j^2\right) \\
&\quad + \frac{1}{6}\epsilon^3\sum_{i\neq j\neq k\neq i} J_{ij}J_{jk}J_{ki}\left(1-m_i^2\right)\left(1-m_j^2\right)\left(1-m_k^2\right) \\
&\quad + \frac{1}{3}\epsilon^3\sum_{i\neq j} J_{ij}^3 m_i\left(1-m_i^2\right)m_j\left(1-m_j^2\right) \\
&\quad + \frac{1}{8}\epsilon^4\sum_{\substack{i\neq j\neq k\neq l\neq i,\\ i\neq k, j\neq l}} J_{ij}J_{jk}J_{kl}J_{li}\left(1-m_i^2\right)\left(1-m_j^2\right)\left(1-m_k^2\right)\left(1-m_l^2\right)
\end{aligned} \tag{50}$$

$$\begin{aligned}
&+\epsilon^4\sum_{i\neq j\neq k\neq i} J_{ik}J_{ij}^2J_{kj}m_i\left(1-m_i^2\right)m_j\left(1-m_j^2\right)\left(1-m_k^2\right) \\
&-\frac{1}{24}\epsilon^4\sum_{i\neq j} J_{ij}^4\left(1-m_i^2\right)\left(1-m_j^2\right)\left(1+3m_i^2+3m_j^2-15m_i^2m_j^2\right).
\end{aligned} \tag{51}$$

This calculation reproduces (with $\epsilon = \beta$) equation (11) of Georges and Yedidia [23] and is in line with equations (9), (10), (14) and (15) in Nakanishi and Takayama [26][3] and the equations (B2)–(B5) in Jacquin and Rançon [47], who derived this result using the Wetterich equation [17].

3. Discussion

We presented a systematic diagrammatic scheme to calculate the effective action for any problem that can be decomposed into a solvable part with known correlators and a perturbing part. We have proved that corrections are composed of two types of diagrams:

- irreducible diagrams in a more general sense than in the Gaussian case: those that cannot be decomposed by detaching a single leg of a vertex;
- diagrams of special form that are neither contained in the perturbation expansions of $\mathcal{Z}$ nor W; they are composed of sub-graphs that are connected by either a vertex $\Gamma_0^{(n)}$, $n \geqslant 2$ that, by at least two legs, connects to a third or higher order bare cumulant. This set of

[3] In comparing the expressions to these works, note the different sum conventions: Georges *et al* and Nakanishi *et al* are only summing over those tuples of distinct indices that lead to different terms, while we allow multiple occurrence of terms already in the definition of the action (35) and correct this by using $\frac{J_{ij}}{2}$ instead of J_{ij} as the interaction. Note that the former sum convention in the second-to-last line of equation (11) in Georges *et al* amounts to a summation over all tuples of three different indices and all even permutations thereof, whereas in equation (15) of Nakanishi *et al*, these permutations are written out explicitly, therefore the summation is only over the tuples with three different indices. Therefore, even if these two expressions seem to disagree by a factor 3 at first sight, they do not, because, depending on the form of the sum, the interpretation of their sum convention changes. We thank Adam Rançon for clarifying this summation convention.

diagrams is found by instantiating a known sequence of skeleton diagrams to the desired order in perturbation theory.

The appearance of the latter diagrams can be regarded as a generalization of the amputation in the Gaussian case, because the inverse propagator $\Gamma_0^{(2)}$ may attach to cumulants of the solvable problem at any order, not only to second order cumulants; only in the latter case it 'amputates' the lines.

The presented inductive proof in addition yields an iterative equation which allows the algebraic construction of all graphs and their combinatorial factors from elementary rules of calculus.

One may wonder why we derived the recursion for Γ based on the ideas of the proof of the linked cluster theorem (see appendix A.3, extending the proof in [2, section 6.1.1] to the non-Gaussian case). It might seem more direct to modify the corresponding proof of one-line irreducibility to the non-Gaussian setting considered here. The latter, however, appeared impossible to us: The elegant proof by Zinn–Justin [2, section 6.5] rests on the assumption that the underlying theory is Gaussian; in their equation (6.59) each line is disconnected in all possible ways and the result is shown to remain connected. The proof hence requires that the only connecting elements of the bare theory be lines; this is precisely the restriction we lift here.

The proof by Weinberg [51, section 16.1] shows elegantly that W decomposes into tree graphs, whose vertices—which one could call 'effective vertices' in this case—are generated by Γ. This statement remains of course true also in the non-Gaussian case, because $W \overset{\mathcal{L}}{\leftrightarrow} \Gamma$ form a pair of Legendre transforms. We use this fact to derive the decomposition into skeleton diagrams. This decomposition also follows directly from the reciprocity relation $1 = \Gamma^{(2)} W^{(2)}$ of the Hessians [2, section 6.2]. The connecting elements in these trees are the full propagators $W^{(2)}$, which Dyson's equation expresses in terms of bare propagators and the self energy. The reciprocity relation implies the recursion for the self-energy $\Gamma_V^{(2)} = -(\Gamma_0^{(2)} + \Gamma_V^{(2)})\, W_V^{(2)}\, \Gamma_0^{(2)}$. Since W_V is composed of all connected graphs, including those containing higher order cumulants of W_0, we see that the terms $\cdots \Gamma_0^{(2)} W_V \Gamma_0^{(2)} \cdots$ appearing in the iteration produce those unusual terms of the form $W_0^{(n\geqslant 2)} \Gamma_0^{(2)} W_0^{(m\geqslant 2)}$ that we found in the general expansion (equation (22)).

An alternative approach is the analog of the Dyson Schwinger equation for the effective action [35, 52, 53], reviewed in [5, section 1.8 and 6.2]. It leads to equations of motion for Γ that enable an iterative expansion, for example in the interaction strength. An iterative solution leads to a proof of the 1PI property in the Gaussian case [5, section 1.8.3]. We believe that the latter approach could be generalized to obtain the same results as presented here. The equation of motion can be derived from the invariance of the integral measure with respect to translations [5, section 1.8.3], but also extends to problems on discrete state spaces, such as the Ising model [5, 21, 22, 32]. From this equation of motion, equation (6.136) in [5] is derived, similar to our (32) with the difference that Vasiliev expands in terms of unperturbed cumulants and not full vertices. Probably, both equations are suitable starting points to rederive our results in section 2.4. The Feynman rules would then be deduced from this step. Possibly these approaches could render the taxonomy of non-standard diagrams clearer. However, it will unlikely be as simple as in the Gaussian case because, as pointed out, reducible non-standard diagrams do not necessarily cancel. We leave this question for future work. In any case, more refined diagrammatic rules previously had to be obtained in a case by case manner so far, depending on the problem at hand (compare also the last paragraph of [5, chapter 6.3.1]). The algorithm presented in section 2.4, in contrast, is the same for any model.

One notes that equation (21) in the work by Vasiliev and Radzhabov [21] is identical to the third order derivation recovered much later by other means [23, 26–28]; in particular the result already includes the TAP approximation [25], if only the first three terms are considered. In principle, these early works [21, 22] also derive the Feynman rules for the Ising model; however, without giving any concrete expression for orders higher than three. In contrast to these results, the set of Feynman rules that we present here are applicable to general non-Gaussian theories. In case of the Ising model these had been sought for some time (see [34, p 28]).

We hope that the presented technique may prove useful in finding new approximations around known limiting cases. Examples may include expansions of the Hubbard model around the atomic limit [23]. An extension of our theory to higher order Legendre transforms, as broadly discussed in [5], could lead to a diagrammatic formulation of the results derived in the context of the inverse Ising problem [46, 47] and to an alternative field-theoretic formulation of the extended Plefka-expansion for stochastic systems, that has recently been developed [54]. The appendix A.6 presents an iterative algorithm as a first step towards this goal, an iterative equation to compute corrections to the second Legendre transform. Further work is required to derive a set of Feynman rules from this equation.

The application of the here presented method is possible whenever a model admits a closed-form solution. An interesting regime of application may therefore be spherical models [55]. In the thermodynamic limit, the free energy, the cumulant-generating function of the model, is known. Extensions of the spherical model that include four point coupling terms for example appear in the field of random lasers [56]. If the quartic term is small compared to the quadratic term, the here proposed method could be applied to obtain approximate self-consistency equations. Such quartic spherical models, moreover, appear in inverse problems of diverse systems [57]. Future work is needed to see if the perturbative results offered by the current work may help at obtaining approximate solutions to such inverse problems.

We also note that the procedure as presented in section 2.4.2 yields a non-iterative way to generate all non-standard diagrams. We believe that this algorithm should be amenable to numerical implementation. The diagrammatic Monte Carlo technique, for example, presents an effective method to calculate the kernels of Schwinger–Dyson equations—for the one-particle Greens function this is the self-energy [58–60]. One way to derive Schwinger–Dyson equations relies on multiple Legendre transforms, expressing the generating functionals in terms of correlation functions instead of potentials, as pioneered by de Dominicis and Martin [7]. The equations of state then constitute self-consistency equations for these correlation functions, such as equation (6.11) in [5]. For example one needs to consider the second Legendre transform to determine the self-energy and the fourth to determine the two-particle Green's function self-consistently. We do a first step towards developing diagrammatic rules for the second Legendre transform in the appendix A.6, whereas higher order Legendre transforms are beyond the scope of the current work. Their diagrammatics is already quite involved if the underlying theory is Gaussian [5, chapter 6.28.f]; the parquet equations form an approximation resulting from the fourth order Legendre transform. A different way, however, to obtain a set of self-consistency equations is by a direct resummation of diagrams, as in the derivation of the Bethe–Salpeter equation [61]. The diagrammatic rules derived here could be useful in such an approach.

In general, the methods also seems particularly promising for hierarchical problems: assuming that a problem can be decomposed into small, but strongly interacting clusters that can be solved exactly, the method may be used to systematically expand in the interaction strength between such clusters.

Acknowledgments

We are indebted to Adam Rançon who commented on an earlier version of this manuscript and especially for his hints on Georges' and Yedidia's summation convention, which allowed us to see that our result is consistent with earlier works. Furthermore, we would like to acknowledge the two anonymous reviewers for many thoughtful comments that helped us to considerably improve the manuscript. In particular, we thank them for pointing out the importance of a non-iterative algorithm, that lead to the idea to use skeleton diagrams, and for pointing us towards literature on spherical models and laser physics as a potential field of application. This work was partly supported by the Exploratory Research Space seed funds MSCALE and CLS002 (partly financed by Hans Herrmann Voss Stiftung) of the RWTH University; the Helmholtz association: Helmholtz young investigator's group VH-NG-1028 'Theory of multi-scale neuronal networks'; European Union's Horizon 2020 framework programme for research and innovation under specific grant agreement No. 785907 (Human Brain Project SGA2), the Jülich Aachen Research Alliance (JARA).

Appendix

A.1. Definition of the effective action

To define the effective action $\Gamma(x^*)$ we eliminate the dependence on the source field j in favor of the mean value $x^*(j) := \langle x \rangle = \partial_j W(j)$ by using (1) and (2) and by following the usual background field method [13, chapter 3.23.6], briefly summarized here: We express W as the integral

$$\exp\left(W(j)\right) = \mathcal{Z}(0)^{-1} \int_x \exp\left(S(x) + j^{\mathrm{T}} x\right) \tag{A.1}$$

and then separate the fluctuations $\delta x = x - x^*$ from the background value x^* to get

$$\exp\left(W(j) - j^{\mathrm{T}} x^*\right) = \mathcal{Z}(0)^{-1} \int_{\delta x} \exp\left(S(x^* + \delta x) + j^{\mathrm{T}} \delta x\right). \tag{A.2}$$

For given x^*, we now choose j in a way that $x^* = \langle x \rangle(j)$ becomes the mean value of the field, so that δx has vanishing mean

$$\begin{aligned} 0 \overset{!}{=} \langle \delta x \rangle &\equiv \mathcal{Z}(0)^{-1} \int_{\delta x} \exp\left(S(x^* + \delta x) + j^{\mathrm{T}} \delta x\right) \delta x \\ &= \mathcal{Z}(0)^{-1} \partial_j \int_{\delta x} \exp\left(S(x^* + \delta x) + j^{\mathrm{T}} \delta x\right) \\ &= \partial_j \exp\left(W(j) - j^{\mathrm{T}} x^*\right), \end{aligned}$$

where we used (A.2) in the last step. Since the exponential function is monotonic, $\exp(x)' > 0 \quad \forall x$, the latter expression vanishes at the point where the exponent is stationary

$$\partial_j \left(W(j) - j^{\mathrm{T}} x^*\right) = 0. \tag{A.3}$$

The condition (A.3) has the form of a Legendre transform (4) from the function $W(j)$ to the effective action $\Gamma(x^*)$. The supremum follows from stationarity (A.3) and because W is convex down, its Hessian $W^{(2)}$, the covariance matrix, is positive definite (see appendix A.2 or [2, p 166]). Therefore, $-W(j) + j^T x^*$, as a function of j, is convex up (concave), so we may define the Legendre transform (4) by the supremum over j.

A.2. Convexity of W

W is convex, because $W^{(2)}$ is the covariance matrix: it is symmetric and therefore has real eigenvalues. For covariance matrices these are in addition always positive [2, p 166]. This can be seen from the following argument. Let us define the bilinear form

$$f(\eta) := \eta^{\mathrm{T}} W^{(2)} \eta.$$

A positive definite bilinear form has the property $f(\eta) > 0 \quad \forall \eta$. With $\delta x := x - \langle x \rangle$ we can express the covariance as $W^{(2)}_{kl} = \langle \delta x_k \delta x_l \rangle$, so we may explicitly write $f(\eta)$ as

$$\begin{aligned} f(\eta) &= \sum_{k,l} \eta_k W^{(2)}_{kl} \eta_l \\ &= \mathcal{Z}^{-1}(j)\, \eta^{\mathrm{T}} \int \mathrm{d}x\, \delta x\, \delta x^{\mathrm{T}}\, \exp\left(S(x) + j^{\mathrm{T}} x\right) \eta \\ &= \mathcal{Z}^{-1}(j) \int \mathrm{d}x\, \left(\eta^{\mathrm{T}} \delta x\right)^2 \exp\left(S(x) + j^{\mathrm{T}} x\right) > 0, \end{aligned}$$

which is the expectation value of a positive quantity.

A.3. Linked cluster theorem

The following proof of connectedness of all diagrammatic contributions to W does not rely on the solvable part S_0 being Gaussian. We here start from the general expression (1) to derive an expansion of $W(j)$, using the definition (2) to write

$$\exp(W(j)) = Z(j) = \exp\left(\epsilon V(\partial_j)\right) \exp\left(W_0(j)\right) \frac{\mathcal{Z}_0(0)}{\mathcal{Z}(0)}. \tag{A.4}$$

Taking the logarithm, the latter factor turns into an additive constant $\ln \frac{\mathcal{Z}_0(0)}{\mathcal{Z}(0)}$ which ensures $W(0) = 0$. Since we are ultimately interested in the derivatives of W, namely the cumulants, we may drop the constant and ensure $W(0) = 0$ by finally dropping the zeroth order Taylor coefficient.

The idea to prove connectedness follows to some extent [2]. The proof is by induction, dissecting the operator $\exp\left(\epsilon V(\partial_j)\right)$ appearing in (A.4) into infinitesimal operators using the definition of the exponential function as the limit

$$\exp\left(\epsilon V(\partial_j)\right) = \lim_{L\to\infty} \left(1 + \frac{\epsilon}{L} V(\partial_j)\right)^L. \tag{A.5}$$

For large L given and fixed and $0 \leqslant l \leqslant L$, we define

$$\exp\left(W_l(j)\right) := \left(1 + \frac{\epsilon}{L} V(\partial_j)\right)^l \exp\left(W_0(j)\right).$$

It fulfills the trivial recursion $\exp(W_{l+1}(j)) = \left(1 + \frac{\epsilon}{L} V(\partial_j)\right) W_l(j)$ from which follows an iteration by multiplication with $\exp(-W_l(j))$ and taking the logarithm

$$W_{l+1}(j) - W_l(j) = \ln\left[\exp\left(-W_l(j)\right) \left(1 + \frac{\epsilon}{L} V(\partial_j)\right) \exp\left(W_l(j)\right)\right]. \tag{A.6}$$

The desired result $W(j)$ then follows as the limit $W(j) = \lim_{L\to\infty} W_L(j)$. Expanding $\ln(1 + \frac{\epsilon}{L} x) = \frac{\epsilon}{L} x + \mathcal{O}\left((\frac{\epsilon}{L})^2\right)$ in (A.6) we get

$$W_{l+1}(j) - W_l(j) = \frac{\epsilon}{L} \left(\exp\left(-W_l(j)\right) V(\partial_j) \exp\left(W_l(j)\right)\right) + O\left(\left(\frac{\epsilon}{L}\right)^2\right). \tag{A.7}$$

We start the induction by noting that for $l = 0$ we have $W_{l=0} = W_0$, the cumulant generating function of the solvable system. At this order, W hence does not contain any diagrammatic corrections; so in particular no disconnected ones.

We assume that the assumption is true until some $0 \leqslant l \leqslant L$. Stated precisely, we assume that all perturbative corrections to $W_l(j)$ with k vertices are connected and are $\propto \left(\frac{\epsilon}{L}\right)^k$; the sub-leading terms $O\left(\left(\frac{\epsilon}{L}\right)^2\right)$ in (A.7) vanish in the limit $L \to \infty$, as shown below. Representing the potential V as a Taylor series, we see that each step adds terms of the form shown in the second line

$$W_{l+1}(j) = 1 \cdot W_l(j) + \frac{\epsilon}{L} \cdot \sum_{\{n_i\}} \frac{V^{(n_1,\ldots,n_N)}}{n_1! \cdots n_N!} \exp\left(-W_l(j)\right) \partial_1^{n_1} \cdots \partial_N^{n_N} \exp\left(W_l(j)\right), \tag{A.8}$$

where ∂_i is used in short for ∂_{j_i}. The Taylor coefficient $\frac{V^{(n_1,\ldots,n_N)}}{n_1! \cdots n_N!}$ is graphically represented by a vertex (see figure 1). Noting that the two exponential factors cancel each other after the differential operator has been applied to the latter factor, what remains is a set of connected components of $W_l(j)$ tied together by the vertex $\frac{V^{(n_1,\ldots,n_N)}}{n_1! \cdots n_N!}$. Disconnected components cannot appear, because there is only a single vertex; each of its legs belongs to one ∂_i, which, by acting on $W_l(j)$, attaches to one leg of the components in W_l.

The iteration (A.8) shows that the second term in each step adds to $W_l(j)$ a set of diagrams to obtain $W_{l+1}(j)$. It is clear from the single appearance of $V^{(n_1,\ldots,n_N)}$ that in each iteration only one such additional vertex is added. We will show now that we only need to consider such additional diagrams, where the new vertex $V^{(n_1,\ldots,n_N)}$ connects to at most one perturbative correction contained in W_l (with $k \geqslant 1$ vertices), while all of its remaining legs connect to a cumulant of the unperturbed theory W_0 (with $k = 0$ vertices). Stated differently, a perturbative correction with k vertices picks up each of its vertices in a different iteration step l in (A.8); contributions where a single iteration step increases the number of vertices in a component by more than one vanish in the $L \to \infty$ limit.

To understand why this is so, we consider the overall factor in front of a resulting diagram with k vertices after L iterations of (A.8). In each step of (A.8) the first term copies all diagrams from W_l. The second term adds those formed by help of the additional vertex $V^{(n_1,\ldots,n_N)}$. Following how one particular graph is generated by the iteration, in each step we have the binary choice to either leave it as it is or to combine it with other components by help of an additional vertex.

We first consider the case that each of the k vertices is picked up in a different step (at different l) in the iteration. Each such step comes with a factor $\frac{\epsilon}{L}$ and in there are $\binom{L}{k}$ ways to select k out of the L iteration steps to pick up a vertex to construct this particular diagram. So in total we get a factor

$$\left(\frac{\epsilon}{L}\right)^k \binom{L}{k} = \frac{\epsilon^k}{k!} \frac{L(L-1)\cdots(L-k+1)}{L^k} \overset{L\to\infty}{\to} \frac{\epsilon^k}{k!}, \tag{A.9}$$

which is independent of L.

Now consider the case that we pick up the k vertices along the iteration (A.8) such that in one step we combined two sub-components with each one or more vertices already. Consequently, to arrive at k vertices in the end, we only need $k' < k$ iteration steps in which the second rather than the first term of (A.8) acted on the component. The overall factor therefore is

$$\left(\frac{\epsilon}{L}\right)^k \binom{L}{k'} = \frac{\epsilon^k}{k'!} \frac{L(L-1)\cdots(L-k'+1)}{L^k}$$
$$\overset{L\gg k'}{=} \frac{\epsilon^k}{k'!} \frac{1}{L^{k-k'}} \overset{L\to\infty}{=} 0. \tag{A.10}$$

We can hence neglect the latter option and conclude that $W(j)$ is composed of all connected graphs, where a perturbative correction with k vertices comes with the factor $\frac{\epsilon^k}{k!}$ given by (A.9). By the same reasoning we may neglect the $O\left(\left(\frac{\epsilon}{L}\right)^2\right)$ term in (A.7), because also here in a single step we would increase the order of the diagram by more than one factor L^{-1}.

A.4. Operator equation for Γ_V

Let us first see why the decomposition into a sum in (11) holds. To this end, we consider (6) with $\delta x = x - x^*$ and use the decomposition (7) of the action as well as the decomposition (11) of Γ to obtain

$$\exp(-\Gamma_0(x^*) - \Gamma_V(x^*)) = \mathcal{Z}^{-1}(0) \int_x \exp\left(S_0(x) + \epsilon V(x) + \left(\Gamma_0^{(1)\mathrm{T}}(x^*) + \Gamma_V^{(1)\mathrm{T}}(x^*)\right)(x - x^*)\right).$$

Collecting the terms depending on x^* on the left hand side we get with (5)

$$\begin{aligned}
&\exp(\underbrace{-\Gamma_0(x^*) + \Gamma_0^{(1)\mathrm{T}}(x^*)\, x^*}_{W_0(j)\big|_{j=\Gamma_0^{(1)}(x^*)}} - \Gamma_V(x^*)) \\
&= \exp\left(\epsilon V(\partial_j) + \Gamma_V^{(1)\mathrm{T}}(x^*)(\partial_j - x^*)\right) \mathcal{Z}^{-1}(0) \int_x \exp\left(S_0(x) + j^{\mathrm{T}}x\right)\Big|_{j=\Gamma_0^{(1)}(x^*)} \\
&= \exp\left(\epsilon V(\partial_j) + \Gamma_V^{(1)\mathrm{T}}(x^*)(\partial_j - x^*)\right) \exp\left(W_0(j)\right)\Big|_{j=\Gamma_0^{(1)}(x^*)},
\end{aligned}$$

where we moved the perturbing potential in front of the integral, making the replacement $x \to \partial_j$ and we identified the unperturbed cumulant generating function $\exp(W_0(j)) = \mathcal{Z}^{-1}(0) \int_x \exp\left(S_0(x) + j^{\mathrm{T}}x\right)$ from the second to the third line. With the term $\Gamma_0^{(1)\mathrm{T}}(x^*)x^* \equiv j_0^{\mathrm{T}}x^*$ on the left hand side, we get $-\Gamma_0(x^*) + j^{\mathrm{T}}x^* = W_0(j)\big|_{j=\Gamma_0^{(1)}(x^*)}$, which follows from the definition (10). Multiplying with $\exp(-W_0(j))\big|_{j=\Gamma_0^{(1)}(x^*)}$ from left then leads to a recursive equation (12) for Γ_V, which shows that our ansatz (11) was indeed justified and that we may determine Γ_V recursively, since Γ_V appears again on the right hand side.

A.5. Recursion for g_l

To construct the diagrams iteratively we write the perturbing term in (12) as

$$\begin{aligned}
&\exp\left(\epsilon V(\partial_j) + \Gamma_V^{(1)\mathrm{T}}(x^*)(\partial_j - x^*)\right) \\
&= \lim_{L\to\infty} \left(1 + \frac{1}{L}\left(\epsilon V(\partial_j) + \Gamma_V^{(1)\mathrm{T}}(x^*)(\partial_j - x^*)\right)\right)^L.
\end{aligned} \tag{A.11}$$

Inserted into (12) we assume L fixed but large and choose some $0 \leqslant l \leqslant L$. We define $G_l(j)$ as the result after application of l factors of the right hand side of (A.11)

$$\exp(G_l(j)) := \left(1 + \frac{1}{L}\left(\epsilon V(\partial_j) + \Gamma_V^{(1)\mathrm{T}}(x^*)\,(\partial_j - x^*)\right)\right)^l \exp(W_0(j)).$$

Obviously we have

$$G_0 \equiv W_0. \tag{A.12}$$

For $l = L \to \infty$, we obtain the desired result as

$$-\Gamma_V(x^*) = \lim_{L\to\infty} G_L(j) - W_0(j)\Big|_{j=\Gamma_0^{(1)}(x^*)}.$$

By its definition, $G_l(j)$ obeys the trivial iteration

$$\exp(G_{l+1}(j)) = \left(1 + \frac{1}{L}\left(\epsilon V(\partial_j) + \Gamma_V^{(1)\mathrm{T}}(x^*)\,(\partial_j - x^*)\right)\right)\exp(G_l(j)).$$

Multiplying from left with $\exp(-G_l(j))$ and taking the logarithm on both sides while using $\ln(1 + \frac{1}{L}x) = \frac{1}{L}x + O(L^{-2})$ we get the recursion for the additional diagrams produced in step $l + 1$

$$\begin{aligned} G_{l+1}(j) - G_l(j) = {} & \frac{\epsilon}{L}\exp(-G_l(j))\,V(\partial_j)\,\exp(G_l(j)) \\ & + \frac{1}{L}\exp(-G_l(j))\,\left(\Gamma_V^{(1)\mathrm{T}}(x^*)\,(\partial_j - x^*)\right)\exp(G_l(j)) \\ & + \mathcal{O}(L^{-2}). \end{aligned} \tag{A.13}$$

By the initial condition (A.12) and the form of the additive iteration (A.13) it is clear that all graphs of W_0 are also contained in G_l for any step l. We may therefore define only the perturbative corrections as $g_l := G_l - W_0$.

We first note that indeed (A.13) yields a closed iteration: Constructing the graphs of up to order $l + 1$ in G_{l+1} by (A.13) we only need the graphs in G_l on the right hand side of (A.13), which, by construction, are of order $\leqslant l$. This is because V contains exactly one bare vertex and $\Gamma_V^{(1)}(x^*)$ contains at least one.

Taken together, we arrive at the central result of our work, equation (13).

A.6. Second Legendre transform

We here extend the iterative procedure to compute perturbative corrections to the second Legendre transform. To this end, we define an effective action that is a function of the first moment x^* and the second moment $c^* = \langle x^2\rangle$. We express W as the integral

$$\exp\left(W(j,k)\right) = \mathcal{Z}(0)^{-1}\int_x \exp\left(S(x) + j^{\mathrm{T}}x + k^{\mathrm{T}}x^2\right). \tag{A.14}$$

Here $k^{\mathrm{T}}x^2$ must be understood as a bilinear form in x, hence $\sum_{il} k_{il}x_i x_l$. We have

$$\frac{\partial W}{\partial j} = \langle x\rangle =: x^*, \qquad \frac{\partial W}{\partial k} = \langle x^2\rangle =: c^*.$$

We would like to define an effective action that is a function of these latter coordinates. So we define $\Gamma(x^*, c^*)$ as

$$\exp\left(-\Gamma(x^*,c^*)\right) = \mathcal{Z}(0)^{-1}\int_x \exp\left(S(x) + j^{\mathrm{T}}(x-x^*) + k^{\mathrm{T}}(x^2-c^*)\right)$$

$$\Gamma(x^*,c^*) = j^{\mathrm{T}}x^* + k^{\mathrm{T}}c^* - W(j,k), \tag{A.15}$$

with the additional constraints that $\partial/\partial j$ and $\partial/\partial k$ of the right hand side vanishes. Consequently, the so-defined function Γ fulfills the two equations of state

$$\frac{\partial\Gamma}{\partial x^*} = j, \qquad \frac{\partial\Gamma}{\partial c^*} = k,$$

which can be obtained by application of the chain rule. The second of these equations, for example, follows as

$$\frac{\partial\Gamma(x^*,c^*)}{\partial c^*} = \frac{\partial j^{\mathrm{T}}}{\partial c^*}x^* + k + \frac{\partial k^{\mathrm{T}}}{\partial c^*}c^* - \underbrace{\frac{\partial W^{\mathrm{T}}}{\partial j}}_{\equiv x^*}\frac{\partial j}{\partial c^*} - \underbrace{\frac{\partial W^{\mathrm{T}}}{\partial k}}_{\equiv c^*}\frac{\partial k}{\partial c^*} = k.$$

Hence we may write the definition of Γ also as

$$\exp\left(-\Gamma(x^*,c^*)\right) = \mathcal{Z}(0)^{-1}\int_x \exp\left(S(x) + \frac{\partial\Gamma^{\mathrm{T}}}{\partial x^*}(x-x^*) + \frac{\partial\Gamma^{\mathrm{T}}}{\partial c^*}(x^2-c^*)\right).$$

We next decompose $S(x) = S_0(x) + \epsilon V(x)$, where we assume that we may compute the cumulant generating function $W_0(j,k) = \ln\int_x \exp(S_0(x) + j^{\mathrm{T}}x + k^{\mathrm{T}}x^2)$ exactly. Correspondingly, we assume a decomposition of the effective action into the solvable part Γ_0 and the perturbative corrections Γ_V as

$$\Gamma(x^*,c^*) = \Gamma_0(x^*,c^*) + \Gamma_V(x^*,c^*).$$

With the notation $\frac{\partial\Gamma}{\partial x^*} =: \Gamma^{(1,0)}$ and $\frac{\partial\Gamma}{\partial c^*} =: \Gamma^{(0,1)}$ we may express the integral equation (A.15) as

$$\begin{aligned}
&\exp(-\Gamma_0(x^*,c^*) - \Gamma_V(x^*,c^*)) \\
&= \mathcal{Z}^{-1}(0)\int_x \exp\Big(S_0(x) + \epsilon V(x) \\
&\qquad + \left(\Gamma_0^{(1,0)\mathrm{T}} + \Gamma_V^{(1,0)}\right)^{\mathrm{T}}(x-x^*) \\
&\qquad + \left(\Gamma_0^{(0,1)\mathrm{T}} + \Gamma_V^{(0,1)}\right)^{\mathrm{T}}(x^2-c^*)\Big)
\end{aligned}$$

or, bringing all terms that are independent of the integration variable x to the left, we get with $j_0 = \Gamma_0^{(1,0)}$ and $k_0 = \Gamma_0^{(0,1)}$

$$\begin{aligned}
&\exp(\underbrace{-\Gamma_0(x^*,c^*) + j_0^{\mathrm{T}}x^* + k_0^{\mathrm{T}}c^*}_{W_0(j_0,k_0)} - \Gamma_V(x^*,c^*)) \\
&= \exp\left(\epsilon V(\partial_j) + \Gamma_V^{(1,0)\mathrm{T}}(\partial_j - x^*) + \Gamma_V^{(0,1)\mathrm{T}}(\partial_k - c^*)\right) \\
&\times \mathcal{Z}^{-1}(0)\int_x \exp\left(S_0(x) + j^{\mathrm{T}}x + k^{\mathrm{T}}x^2\right)\Big|_{j=\Gamma_0^{(1,0)}(x^*,c^*),\, k=\Gamma_0^{(0,1)}(x^*,c^*).}
\end{aligned}$$

We hence obtain the operator form of the equation as

$$\begin{aligned}\exp(-\Gamma_V(x^*,c^*)) = \exp(-W_0(j,k)) \\ \times \exp\left(\epsilon V(\partial_j) + \Gamma_V^{(1,0)\mathrm{T}}(\partial_j - x^*) + \Gamma_V^{(0,1)\mathrm{T}}(\partial_k - c^*)\right) \\ \times \exp(W_0(j,k))\big|_{j=\Gamma_0^{(1,0)}(x^*,c^*),k=\Gamma_0^{(0,1)}(x^*,c^*)}.\end{aligned}$$

Using the representation of the exponential function as a series and the series expansion of the logarithm to first order, we get the iteration

$$\begin{aligned}g_{l+1}(j,k) - g_l(j,k) = \frac{\epsilon}{L}\exp(-W_0(j,k) - g_l(j,k))\, V(\partial_j)\, \exp(W_0(j,k) + g_l(j,k)) \\ + \frac{1}{L}\exp(-W_0(j,k) - g_l(j,k))\, \Gamma_V^{(1,0)}\, (\partial_j - x^*)\, \exp(W_0(j,k) + g_l(j,k)) \\ + \frac{1}{L}\exp(-W_0(j,k) - g_l(j,k))\, \Gamma_V^{(0,1)}\, (\partial_k - c^*)\, \exp(W_0(j,k) + g_l(j,k)) \\ + \mathcal{O}(L^{-2}),\end{aligned} \tag{A.16}$$

with the initial condition $g_0 = 0$. The perturbative corrections to the effective action then result as the limit

$$-\Gamma_V(x^*,c^*) = \lim_{L\to\infty} g_L(j,k)\Big|_{j=\Gamma_0^{(1,0)}(x^*,c^*),\, k=\Gamma_0^{(0,1)}(x^*,c^*)}.$$

One could use this iterative procedure to compute perturbative corrections. It seems that a proof of a generalized irreducibility should follow along similar lines as in the case of a first order Legendre transform. In particular, the term $\Gamma_V^{(0,1)}\,(\partial_k - c^*)$ establishes a double link between a component contained in g_l and one in Γ_V, thus suggesting a more general 2PI property. We will leave a more careful consideration open for subsequent works.

A.7. Taxonomy of reducible diagrams

One might wonder why the diagram in figure 4(c) remains in the perturbative expansion of Γ despite being reducible in the sense that it is divided into two parts by cutting one of the legs of $\Gamma_0^{(2)}$, which otherwise acts similarly as a leg of a bare interaction vertex. We here provide an explanation in the framework of the iterative construction of Γ_V. There are four different types of diagrams that are reducible in the sense that they fall apart if one detaches one leg from a cumulant. We classify them by the type of subdiagrams (leaves) they are composed of and how these leaves are connected. We can distinguish five cases:

- I Two irreducible diagrams from W_V connected by a single leg that belongs to a bare interaction vertex.
- Ia Multiple irreducible diagrams from W_V that are connected to the remainder by the same junction as in case I.
- II Two irreducible diagrams from $W_V^{(1)}$ connected via a $\Gamma_0^{(2)}$-component.
- III One diagram from $W_V^{(1)}$ and one non-standard component of Γ_V (not contained in the expansion of W_V), necessarily connected by a $\Gamma_0^{(n)}$-component
- IV Two non-standard diagrams of Γ_V (not contained in the expansion of W_V), necessarily connected by a $\Gamma_0^{(n)}$-component

In case I, in which both parts are irreducible, we may insert either one or two unities of the form

$1 =$ 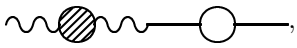 , (A.17)

where empty and hatched circles in this section always denote the unperturbed quantities $W_0^{(n)}$ and $\Gamma_0^{(2)}$, respectively. We therefore see that we can replace both leaves by a part of $\Gamma_V^{(1)}(x^*)$. So, together with the original diagram, we have four contributions that all contribute with the same magnitude, two of them positive, two of them negative: The sum is 0. Schematically, the situation is as follows:

$0 =$ 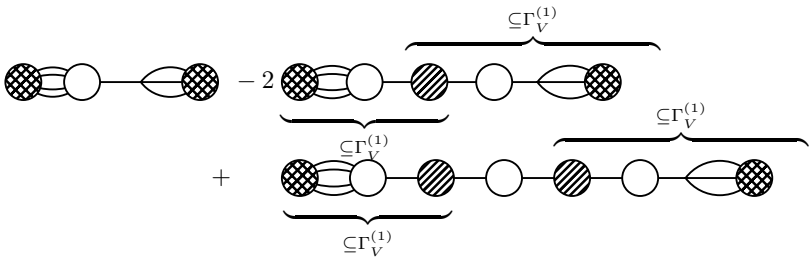

Here the circles filled with squares denote some arbitrary continuation of the respective diagram. We conclude that in second order in the interactions, no diagrams with irreducible $W_V^{(1)}$-leaves contribute. We will proof by induction in the number of vertices n that no diagram described in case Ia (with at least one reducible link) contributes to Γ_V. Case I is our induction assumption ($n = 2$). Assume that the assumption holds $\forall\, k \leqslant n$. We observe that if the whole diagram contains $n + 1$ interactions we can pick an arbitrary leaf that is connected to the rest by a single link, so that the (reducible) rest contains at most n interactions. By the induction assumption, this rest is not contained in the diagrammatic expansion of Γ_V. Therefore, we just have one contribution, which can be replaced by a part of $\Gamma_V^{(1)}$ contributing with opposite sign. This contribution cancels the contribution constructed solely out of bare vertices. Diagrammatically this could be depicted by

$0 =$ 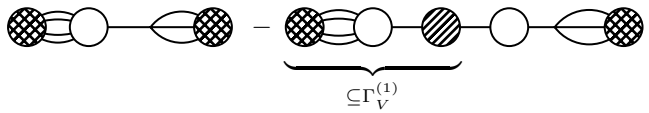

This concludes the induction. We conclude from these observations that no diagrams with a single irreducible $W_V^{(1)}$-leaf contribute.

Considering case II, it is obvious that we can choose one of the leaves to be provided by $\Gamma_V^{(1)}$ and the other one to be composed of bare vertices. We can also insert a unity (A.17) to the left of the given $\Gamma_0^{(2)}$, so that we can interpret both leaves to come from $\Gamma_V^{(1)}(x^*)$. Because the diagram composed solely of bare vertices is missing, we only have three contributions. They all contribute with the same absolute value, but two of them with one sign, one with the other sign and therefore, the contributions do not sum to zero and the whole diagram contributes to the expansion of Γ_V, as claimed in the main text. Diagrammatically, this is illustrated by

$0 \neq -2 \cdot$ 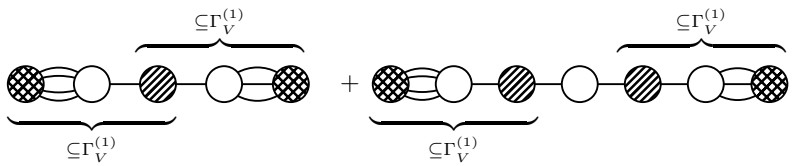

. (A.18)

In point II, we have proved that there are diagrams contributing to Γ_V, but not to W_V (for the example figure 4(c)), therefore the situations of points III and IV can appear.

The diagrams described under point III cancel, because the irreducible components within the $W_V^{(1)}$-like leaf can be replaced a $\Gamma_V^{(1)}$-part or can be left as it is. Both contribute with same absolute value, but opposite sign and cancel. Because the other part cannot be composed just by bare vertices and unperturbed cumulants, it occurs only once, namely as part of $\Gamma_V^{(1)}$. Therefore, the contribution from this diagram remains zero.

Point IV is even simpler, because by construction we only have a unique way to construct the composed diagram, namely by joining two $\Gamma_V^{(1)}$-parts and therefore, the whole diagram is not canceled.

Using these rules to determine if a given diagram contributes to Γ_V or not, we conclude from case Ia that, as mentioned in the main text, diagrams with at least one component from W_V do not contribute. However, one has to be careful applying case III to rule out the occurrence of a certain diagram, that can be decomposed according to III, because this decomposition is not necessarily unique and so the contribution of the whole diagram is actually not zero.

A.8. Calculation of symmetry factors in the diagrammatic solution of the Ising model

We determine here the symmetry factors of the diagrams given in the main text using the following scheme: First, label all legs of interactions by indices. Then, count the possible combinations of swaps of the two legs at an interaction and permutations of interactions that lead to a new labeled diagram.

For the second-order-diagram (42), this is just 2 coming from the fact that flipping a single vertex produces a new labeled diagram, but flipping both vertices leaves the diagram invariant.

For the ring diagram in third order (43), permuting interactions produces the same diagram ('at most' it mirrors the diagram). The same holds for the other third order diagram (44).

Swapping legs in the last diagram (44) yields a factor 2^2, because switching all vertex legs does not yield a new labeled diagram, whereas for the ring diagram, it does, leading to the symmetry factor 2^3.

Proceeding to fourth order, we first compute the symmetry factor S_R of the ring diagram in (45). For a given interaction, we have 3 possibilities to choose another interaction *not* to pair it with and every vertex flip produces a new labeled diagram. This gives $S_\mathrm{R} = 3 \cdot 2^4 = 48$.

For the second diagram (46), labeled by 'TM' (because it is depicted in a hexagonal shape reminiscent of the elements of the game board of 'Terra Mystica'), we may choose $\binom{4}{2}$ vertices for the upper position and flip every of the four vertices: $S_\mathrm{TM} = 6 \cdot 2^4 = 96$.

The diagram (47) that looks like a doubled Citroën logo (dC), whose symmetry factor is given—analogous to its third-order-counterpart—by $S_\mathrm{dC} = 2^3 = 8$. Including the numerical factors contained in the third-oder-cumulants into the prefactor, we end up with the following contribution to the effective action:

$$\frac{1}{16} \underbrace{\frac{8 \cdot (-2)^2}{24}}_{=\frac{4}{3}} \sum_{i \neq j} J_{ij}^2 J_{jk}^2 \left(1 - m_i^2\right) \left(1 - m_j^2\right) \left(1 - 3m_i^2\right) \left(1 - 3m_j^2\right). \tag{A.19}$$

Finally, let us determine the symmetry factors for the 'non-standard' fourth-order-contributions in (48), S_i for $i \in \{a, b, c\}$: For diagram a, which we term 'glasses'-diagram for obvious reasons, there are three ways to pair, say, the first vertex with any of the three others. The other

pair is then fixed, too. Then, every flip of a vertex produces a new labeled diagram because it matters which vertex is attached to the four-point-cumulant. Together, this gives $S_a = 3 \cdot 2^4$.

For diagram S_b, flipping each of the two single vertices in the left part produces a new labeled diagram, because it matters which vertex is attached to the three-point-cumulant (2^2). The leaf brings in a factor 2, because also here, flipping both vertices brings in a factor 2 each and a factor 1/2 because the leaf is of second order in the interaction. We count the leaf as a different interaction type, therefore the prefactor is given by $\frac{2^3}{2!\cdot 1!}$.

Finally, there is only one way to construct diagram c and we are left with the intrinsic symmetry factors of the clusters: $S_c = 2^2$. Here again, $\Gamma_V^{(1)}$ acts as a special kind of interaction, which occurs twice, which leads to the prefactor $\frac{2^2}{2}$. Adding up the contributions of the three diagrams leads us to the following expression for the term inside the square bracket in (48):

$$\begin{aligned}&\left\{\frac{1}{4!}3\cdot 2^4\,(-2)\left(1-3m_j^2\right)+\left(-\frac{1}{2!1!}8+\frac{1}{2}4\right)4m_j^2\right\}\left(1-m_i^2\right)\left(1-m_j^2\right)\left(1-m_k^2\right)\\ &=\left\{-4\left(1-m_j^2\right)\right\}\left(1-m_i^2\right)\left(1-m_j^2\right)\left(1-m_k^2\right).\end{aligned} \tag{A.20}$$

In conclusion, the diagrams in (48) add up to

$$\frac{-4}{2^4}\sum_{i\neq j\neq k}J_{ij}^2J_{jk}^2\left\{1-m_j^2\right\}\left(1-m_i^2\right)\left(1-m_j^2\right)\left(1-m_k^2\right). \tag{A.21}$$

The term in curly braces, despite emerging from a sum of three different diagrams, looks like a second cumulant. Interestingly, the contribution (A.21) for the case $i \neq k$ is exactly canceled by that of the ring-diagram in the case that the indices of exactly two of the opposite cumulants in the ring are equal. We see this as follows: There are two ways how exactly two indices of opposite circles in the ring can be identified ($i = k$ or $j = l$) so that the symmetry factor of this diagram is multiplied by 2, which gives the total prefactor $\frac{1}{4!}\frac{1}{2^4}S_{\mathrm{R}}\cdot 2 = \frac{1}{4}$, which is indeed equal to the prefactor in (A.21) (up to the sign). Similarly, we get a contribution to the case of only two different indices in addition to the 'double Citroën-diagram'. For the diagrams S_a, S_b, and S_c that means that the indices of the outer circles are equal, giving the contribution

$$-\frac{1}{4}\sum_{i\neq j}J_{ij}^2J_{jk}^2\left(1-m_i^2\right)^2\left(1-m_j^2\right)^2. \tag{A.22}$$

For the ring diagram, there is a unique way to identify indices of opposite circles, therefore we do not get the factor 2 in addition to the symmetry factor such that this contribution does not cancel (A.22), but just reduces it to $-\frac{1}{16}2\sum_{i\neq j}J_{ij}^2J_{jk}^2\left(1-m_i^2\right)^2\left(1-m_j^2\right)^2$. The 'quadruple Citroën-diagram' (47) gives us (A.19). Adding up the relevant terms of these two contributions, leaving out common factors and the summation, gives

$$\begin{aligned}&-2\left(1-m_i^2\right)^2\left(1-m_j^2\right)^2+\frac{4}{3}\left(1-m_i^2\right)\left(1-m_j^2\right)\left(1-3m_i^2\right)\left(1-3m_j^2\right)\\ &=\frac{2}{3}\left(1-m_i^2\right)\left(1-m_j^2\right)\left(-3\left(1-m_i^2\right)\left(1-m_j^2\right)+2\left(1-3m_i^2\right)\left(1-3m_j^2\right)\right)\\ &=\frac{2}{3}\left(1-m_i^2\right)\left(1-m_j^2\right)\left(-1-3m_i^2-3m_j^2+15m_i^2m_j^2\right).\end{aligned} \tag{A.23}$$

Taken together this leads to (49).

ORCID iDs

Tobias Kühn https://orcid.org/0000-0003-0741-1083
Moritz Helias https://orcid.org/0000-0002-0404-8656

References

[1] Negele J W and Orland H 1998 *Quantum Many-Particle Systems* (New York: Perseus Books)
[2] Zinn-Justin J 1996 *Quantum Field Theory and Critical Phenomena* (Oxford: Clarendon)
[3] Amit D J 1984 *Field Theory, the Renormalization Group, and Critical Phenomena* (Singapore: World Scientific)
[4] Altland A and Simons B 2010 *Concepts of Theoretical Solid State Physics* (Cambridge: Cambridge University Press)
[5] Vasiliev A 1998 *Functional Methods in Quantum Field Theory and Statistical Physics* (London: Gordon and Breach)
[6] Mayer J E and Geoppert-Mayer M 1977 *Statistical Mechanics* 2nd edn (New York: Wiley)
[7] De Dominicis C and Martin P C 1964 *J. Math. Phys.* **5** 14
[8] Lasinio J 1964 *Nuovo Cimento* **34** 1790
[9] Goldstone J, Salam A and Weinberg S 1962 *Phys. Rev.* **127** 965–70
[10] Berges J, Tetradis N and Wetterich C 2002 *Phys. Rep.* **363** 223–386 (Renormalization group theory in the new millennium. {IV})
[11] Sénéchal D, Tremblay A and Bourbonnais C 2004 *Theoretical Methods for Strongly Correlated Electrons* (New York: Springer)
[12] Fock V 1930 *Z. Phys.* **61** 126–48
[13] Kleinert H 2009 *Path Integrals in Quantum Mechanics, Statistics, Polymer Physics, and Financial Markets* 5th edn (Singapore: World Scientific)
[14] Wilson K G and Kogut J 1974 *Phys. Rep.* **12** 75–199
[15] Wilson K G 1975 *Rev. Mod. Phys.* **47** 773–840
[16] Hertz J A 1976 *Phys. Rev.* B **14** 1165
[17] Wetterich C 1993 *Phys. Lett.* B **301** 90–4
[18] Metzner W, Salmhofer M, Honerkamp C, Meden V and Schönhammer K 2012 *Rev. Mod. Phys.* **84** 299–352
[19] Gardiner C W 1985 *Handbook of Stochastic Methods for Physics, Chemistry and the Natural Sciences* (*Springer Series in Synergetics* vol 13) 2nd edn (Berlin: Springer)
[20] Uhlenbeck G E and Ford G W 1963 *Lectures in Statistical Physics* (Providence, RI: American Mathematical Society)
[21] Vasiliev A N and Radzhabov R A 1974 *Theor. Math. Phys.* **21** 963–70
[22] Vasiliev A N and Radzhabov R A 1975 *Theor. Math. Phys.* **23** 575–9
[23] Georges A and Yedidia J S 1991 *J. Phys. A: Math. Gen.* **24** 2173
[24] Kirkpatrick S and Sherrington D 1978 *Phys. Rev.* B **17** 4384
[25] Thouless D J, Anderson P W and Palmer R G 1977 *Phil. Mag.* **35** 593–601
[26] Nakanishi K and Takayama H 1997 *J. Phys. A: Math. Gen.* **30** 8085–94
[27] Tanaka T 1998 *Phys. Rev.* E **58** 2302–10
[28] Plefka T 1982 *J. Phys. A: Math. Gen.* **15** 1971–8
[29] Sommers H 1987 *Phys. Rev. Lett.* **58** 1268–71
[30] Horwitz G and Callen H B 1961 *Phys. Rev.* **124** 1757–85
[31] Bloch C and Langer J 1965 *J. Math. Phys.* **6** 554–72
[32] Bogolyubov N M, Brattsev V F, Vasiliev A N, Korzhenevskii A L and Radzhabov R A 1976 *Theor. Math. Phys.* **26** 230–7
[33] Yedidia J S and Georges A 1990 *J. Phys. A: Math. Gen.* **23** 2165
[34] Opper M and Saad D (ed) 2001 *Advanced Mean Field Methods—Theory and Practice* (Cambridge, MA: MIT Press)
[35] Dahmen H D and Jona-Lasinio G 1967 *Il Nuovo Cimento* A **52** 807–38
[36] Hopfield J J 1982 *Proc. Natl Acad. Sci.* **79** 2554–8
[37] Gabrié M, Tramel E W and Krzakala F 2015 Training restricted boltzmann machines via the thouless-anderson-palmer free energy *Proc. 28th Int. Conf. on Neural Information Processing Systems—Volume 1* (Cambridge, MA: MIT Press) pp 640–8

[38] Carreira-Perpiñán M A and Hinton G E 2005 On contrastive divergence learning *Artif. Intell. Stat.* 8
[39] Smolensky P 1986 Information processing in dynamical systems: foundations of harmony theory *Parallel Distributed Processing: Explorations in the Microstructure of Cognition* vol 1 ed D E Rumelhart *et al* (Cambridge, MA: MIT Press) pp 194–281
[40] Hinton G E and Salakhutdinov R R 2006 *Science* **313** 504–7
[41] Tkačik G, Schneidman E, Berry M II and Bialek W 2006 arXiv:q–bio/0611072
[42] Roudi Y, Tyrcha J and Hertz J 2009 *Phys. Rev.* E **79** 051915
[43] Hertz J, Roudi Y and Tyrcha J 2011 arXiv:1106.1752
[44] Nguyen H C, Zecchina R and Berg J 2017 *Adv. Phys.* **66** 197–261
[45] Kappen H, Rodríguez F and Rodríguez F B 1998 Boltzmann machine learning using mean field theory and linear response correction *Advances in Neural Information Processing Systems* (Cambridge, MA: MIT Press) pp 280–6
[46] Sessak V and Monasson R 2009 *J. Phys. A: Math. Theor.* **42** 055001
[47] Jacquin H and Rançon A 2016 *Phys. Rev.* E **94** 042118
[48] Roudi Y, Aurell E and Hertz J A 2009 *Front. Comput. Neurosci.* **3** 22
[49] Schneidman E, Berry M J, Segev R and Bialek W 2006 *Nature* **440** 1007–12
[50] Tkačik G, Marre O, Amodei D, Schneidman E, Bialek W and Berry M J II 2014 *PLoS Comput. Biol.* **10** e1003408
[51] Weinberg S 2005 *The Quantum Theory of Fields—Volume* II (Cambridge: Cambridge University Press)
[52] Vasiliev A N and Kazanskii A K 1973 *Theor. Math. Phys.* **14** 215–26
[53] Vasiliev A N, Kazanskii A K and Pis'mak Y M 1974 *Theor. Math. Phys.* **19** 443–53
[54] Bravi B, Sollich P and Opper M 2016 *J. Phys. A: Math. Theor.* **49** 194003
[55] Berlin T H and Kac M 1952 *Phys. Rev.* **86** 821–35
[56] Antenucci F, Crisanti A and Leuzzi L 2015 *Phys. Rev.* A **91** 053816
[57] Marruzzo A, Tyagi P, Antenucci F, Pagnani A and Leuzzi L 2017 *Sci. Rep.* **7** 3463
[58] Greitemann J and Pollet L 2018 *SciPost Phys. Lect. Notes* 2
[59] Van Houcke K, Werner F, Kozik E, Prokofiev N, Svistunov B, Ku M J H, Sommer A T, Cheuk L W, Schirotzek A and Zwierlein M W 2012 *Nat. Phys.* **8** 366
[60] Van Houcke K, Kozik E, Prokofiev N and Svistunov B 2008 arXiv:0802.2923
[61] Salpeter E E and Bethe H A 1951 *Phys. Rev.* **84** 1232–42